

## The Rate and Spatial Distribution of Novae in M31 as Determined by a Twenty-Year Survey

TRAVIS A. RECTOR <sup>1,\*</sup> ALLEN W. SHAFTER <sup>2</sup> WILLIAM A. BURRIS <sup>2</sup> MATTHEW J. WALENTOSKY,<sup>1</sup>  
KENDALL D. VIAFORE,<sup>1</sup> ALLISON L. STROM <sup>1</sup> RICHARD J. COOL,<sup>3</sup> NICOLE A. SOLA,<sup>1</sup> HANNAH CRAYTON,<sup>1</sup>  
CATHERINE A. PILACHOWSKI <sup>4</sup> GEORGE H. JACOBY <sup>5</sup> DANIELLE L. CORBETT,<sup>3</sup> MICHELLE RENE,<sup>3</sup> AND  
DENISE HERNANDEZ<sup>3</sup>

<sup>1</sup>University of Alaska Anchorage, Department of Physics & Astronomy, Anchorage, AK 99508, USA

<sup>2</sup>San Diego State University, Department of Astronomy, San Diego, CA 92182, USA

<sup>3</sup>Steward Observatory, The University of Arizona, 933 N. Cherry Ave., Tucson, AZ 85721, USA

<sup>4</sup>Astronomy Department, Indiana University Bloomington, Swain West 318, 727 East Third Street, Bloomington, IN 47405-7105, USA

<sup>5</sup>National Optical Astronomy Observatory (NOAO), 950 N. Cherry Ave., Tucson, AZ 85719, USA

### ABSTRACT

A long-term (1995–2016) survey for novae in the nearby Andromeda galaxy (M31) was conducted as part of the Research-Based Science Education initiative. During the course of the survey 180 nights of observation were completed at Kitt Peak, Arizona. A total of 262 novae were either discovered or confirmed, 40 of which have not been previously reported. Of these, 203 novae form a spatially-complete sample detected by the KPNO/WIYN 0.9-m telescope within a  $20' \times 20'$  field centered on the nucleus of M31. An additional 50 novae are part of a spatially-complete sample detected by the KPNO 4-m telescope within a larger  $36' \times 36'$  field. Consistent with previous studies, it is found that the spatial distribution of novae in both surveys follows the bulge light of M31 somewhat more closely than the overall background light of the galaxy. After correcting for the limiting magnitude and the spatial and temporal coverage of the surveys, a final nova rate in M31 is found to be  $R = 40_{-4}^{+5} \text{ yr}^{-1}$ , which is considerably lower than recent estimates. When normalized to the  $K$ -band luminosity of M31, this value yields a luminosity-specific nova rate,  $\nu_K = 3.3 \pm 0.4 \text{ yr}^{-1} [10^{10} L_{\odot,K}]^{-1}$ . By scaling the M31 nova rate using the relative infrared luminosities of M31 and our Galaxy, a nova rate of  $R_G = 28_{-4}^{+5}$  is found for the Milky Way.

*Keywords:* Cataclysmic variable stars (203) – Classical Novae (251) – Galaxies (573) – Novae (1127)  
– Time Domain Astronomy (2109)

### 1. INTRODUCTION

Novae are transient sources that arise from a thermonuclear runaway on the surface of an accreting white dwarf in a close binary system (see Warner 1995; Starfield et al. 2016, and references therein). Their eruptions are believed to play a significant role in the chemical evolution of galaxies, particularly with regard to the production of the isotopes of some light elements such

as  ${}^7\text{Li}$  and CNO group nuclei (see Della Valle & Izzo 2020, for a recent review).

The eruptions of novae do not disrupt the progenitor binary, and as a result, continued accretion onto the white dwarf produces recurrent outbursts on timescales from approximately a year up to of order  $10^5$  yr. Despite the fact that all novae are recurrent, only systems with the shortest recurrence times, and where more than one eruption has been recorded, are referred to explicitly as Recurrent Novae.

The eruptions of novae are among the most luminous of any optical transients, with absolute magnitudes ranging from  $M_V \simeq -5$  to  $M_V \simeq -10$  for the most luminous systems (e.g., Shafter et al. 2009). Their high luminosities make novae easily visible in nearby galaxies, where they can serve as tracers of the close binary star content across differing stellar populations.

Corresponding author: Travis A. Rector  
tarector@alaska.edu

\* National Optical Astronomy Observatory (NOAO), 950 N. Cherry Ave., Tucson, AZ 85719. Visiting astronomer, Kitt Peak National Observatory at NSF's NOIRLab, managed by the Association of Universities for Research in Astronomy (AURA) under a cooperative agreement with the National Science Foundation.

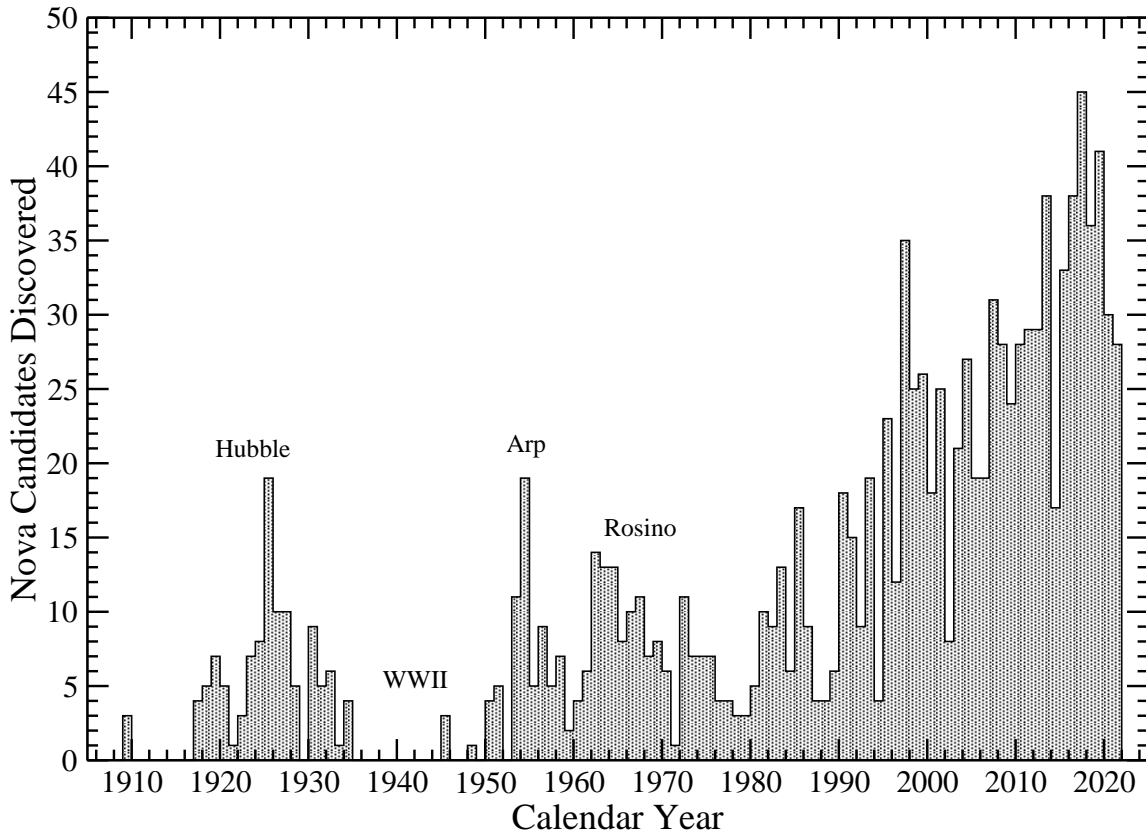


**Figure 1.** The number of nova candidates discovered in M31 in a given calendar year spanning the past 113 years. The average annual number of candidates detected during the seven-year period between 2016 and 2021 was 36. Assuming these candidates are all bona fide novae, this number would appear to place a stringent lower limit to the nova rate in M31.

The observed properties of novae, in particular their peak luminosity, the rate of decline from maximum light, and their rate of recurrence is primarily a function of the mass of the white dwarf, its rate of accretion, and the chemical composition of the gas from the companion star being pulled onto its surface (e.g., Nomoto 1982; Townsley & Bildsten 2005; Kato et al. 2014; Starrfield et al. 2016). Given that these properties of the progenitor binary are expected to vary with the underlying stellar population from which the novae arise, it is reasonable to expect that the nova rate and light curve properties of novae should similarly vary between differing stellar populations and Hubble types. Although novae have now been detected in more than a dozen extragalactic systems, it is still unclear whether and how the observed properties of novae differ between these galaxies (e.g., see Shafter et al. 2014; Shafter 2019; Della Valle & Izzo 2020, and references therein).

More novae have been observed in M31 than all other external galaxies combined. Discoveries of M31 novae go back more than a century, with the first novae reported by Ritchey (1917) during the course of a survey undertaken with the 60-in reflector on Mount Wilson<sup>1</sup>. Since the first nova was discovered on 1909 September 12 (M31N 1909-09a), more than 1200 additional nova candidates have been identified in M31. Many of these objects were discovered as part of targeted surveys beginning with Hubble’s classic study (Hubble 1929).

After a hiatus of more than two decades spanning the great Depression and war years, two additional photographic surveys were initiated. The first of these was un-

<sup>1</sup> Not including S Andromeda (Nova Andromeda 1885), the supernova that was misidentified as a nova before the distinction between the two was finally appreciated in the 1930s.

dertaken (with Hubble’s encouragement) by [Arp \(1956\)](#). Arp discovered a total of 30 novae during the period between June 1953 and January 1955. The second, and last of the major photographic surveys was conducted by Rosino and collaborators with the 1.22-m and 1.82-m reflectors at the Asiago and Ekar observatories in northern Italy. Their observations spanned several decades beginning in the mid 1950s and continuing until 1986 ([Rosino 1964, 1973; Rosino et al. 1989](#)).

By the time the Rosino survey was concluding, modern digital surveys were becoming the standard (e.g., [Ciardullo et al. 1987; Shafter & Irby 2001; Darnley et al. 2006](#)). These surveys, coupled in recent years with the ever-increasing contributions from amateur astronomers and the proliferation of automated telescopes such as the Zwicky Transient Facility (ZTF, [Bellm et al. 2019](#)), have led to a substantial increase in the number of nova candidates discovered in M31 each year (see [Figure 1](#)).

Despite the wealth of data, a reliable estimate for the annual rate of novae in M31 has remained elusive, with estimates over the past century ranging from as few as  $26 \text{ yr}^{-1}$  ([Arp 1956](#)) to in excess of  $100 \text{ yr}^{-1}$  in the case of model simulations ([Soraisam et al. 2016; Chen et al. 2016](#)). These estimates have often been made from surveys with limited temporal coverage and numbers of detected novae. For example, the most recent and widely-accepted estimate of  $65_{-15}^{+16} \text{ yr}^{-1}$  ([Darnley et al. 2006](#)) is based upon the detection of just 20 novae over the course of a 4-year survey.

In this paper we describe an intensive, long-term program to study the novae population in M31. Spanning more than two decades between the years of 1995 and 2016, observations in search of novae in M31 were undertaken as part of the Research-Based Science Education (RBSE) project conducted at Kitt Peak National Observatory (KPNO). RBSE is a course-based undergraduate research experience (CURE), wherein students participate in an authentic research project as part of an introductory class ([Rector et al. 2019](#)). Student gains in understanding the scientific process from participating in RBSE are described in [Wooten et al. \(2018\)](#). The RBSE observations, which resulted in the detection of 262 individual novae, provide a rich dataset with which to study the properties of novae in M31, including their spatial distribution and overall rate. Here, we present the results of the RBSE survey.

## 2. OBSERVATIONS

For the purposes of this paper, all observations of M31 completed on a single night were combined into one image, representing a single epoch. A total of 180 epochs were completed from 1995 September 3 to 2016 October 22. Within the constraints of scheduling and weather, observations were attempted on a monthly basis from 1997 through 2011 during the July-January time period when M31 is accessible. To search for novae that fade rapidly, several campaigns were undertaken in which

M31 was observed on a nightly basis for the span of one or more weeks.

All but 15 of the 180 epochs were observed with the KPNO/WIYN 0.9-m telescope<sup>2</sup>. Supplemental observations were obtained with the KPNO *Mayall* 4-m telescope, the KPNO 2.1-m telescope, the *Bok* 90-in telescope at Steward Observatory<sup>3</sup>, and the *McGraw-Hill* 1.3-m telescope at the MDM Observatory<sup>4</sup>. Observations from the *Local Group Survey* (LGS) ([Massey et al. 2006](#)) were also used. Multiple cameras were used on the telescopes, with the technical details for each camera and telescope configuration given in [Table 1](#).

Following the pioneering study of [Ciardullo et al. \(1987\)](#), we chose to conduct the RBSE survey by imaging in H $\alpha$ . Shortly after eruption novae develop strong and broad H $\alpha$  emission lines that persist long after the continuum has faded. Thus H $\alpha$  observations have a distinct advantage in synoptic surveys with sporadic temporal coverage. In addition, H $\alpha$  observations provide a better contrast against the bright background of the galaxy’s bulge where the nova density is highest.

Prior M31 nova surveys in H $\alpha$  (e.g., [Ciardullo et al. 1987; Shafter & Irby 2001](#)) have shown that a survey with a limiting absolute magnitude of  $M_{\text{H}\alpha} \sim -7.5$  is sufficiently deep to detect a typical nova several months after eruption.<sup>5</sup> With the 0.9-m telescope it is possible to reach this depth with a total integration time of 30 min. Multiple observations with small offsets were made between exposures to minimize the effects of bad pixels, cosmic rays, and transient objects (e.g., asteroids and satellite trails). For single-CCD cameras on the 0.9-m telescope (t2ka, s2kb, and HDI), this was achieved with three 10-min exposures. For observations with the multi-CCD Mosaic camera, five 6-min exposures were used to facilitate filling in chip gaps. To avoid saturating the standard stars, integration times were shortened to five 5-min exposures with the 90-in telescope and five 3-min exposures with the 4-m telescope. The KPNO 2.1-m telescope and the MDM 1.3-m telescope were used only once each. Because of their smaller fields of view, a mosaic of pointings was taken to produce an effective FOV of  $23' \times 23'$  for each epoch, matching the 0.9-m/t2ka configuration. The details of each epoch of observations are given in [Table 2](#). The number of epochs per year is shown in [Figure 2](#). The distribution of time

<sup>2</sup> The WIYN Observatory is a joint facility of the NSF’s National Optical-Infrared Astronomy Research Laboratory, Indiana University, the University of Wisconsin-Madison, Pennsylvania State University, the University of Missouri, the University of California-Irvine, and Purdue University.

<sup>3</sup> Steward Observatory is operated by the University of Arizona.

<sup>4</sup> MDM Observatory is operated by a consortium of Dartmouth College, The Ohio State University, Columbia University, the University of Michigan, and Ohio University.

<sup>5</sup> The H $\alpha$  magnitude is defined on the AB system where  $m_{\text{H}\alpha} = 0$  for  $f_{\lambda} = 2.53 \times 10^{-9} \text{ ergs cm}^{-2} \text{ s}^{-1} \text{ \AA}^{-1}$ .

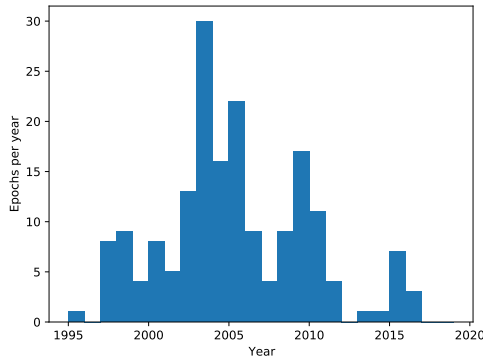
**Table 1.** Telescope and Detector Characteristics

Telescope/ Detector	Scale (" pix <sup>-1</sup> )	FOV (' on a side)	Epochs (nights)
0.9-m/t2ka	0.68	23	20
0.9-m/MOSA	0.43	59	41
0.9-m/s2kb	0.60	20	96
0.9-m/HDI	0.43	29	9
1.3-m/Echelle	0.50	17	1
2.1-m/t2ka	0.31	10	1
Bok/90prime	0.45	70	5
4-m/MOSA	0.26	36	7

**Table 2.** List of Observations

Date (UT)	Date (MJD)	Telescope/ Detector	Seeing (")
1995-09-03	49963.26	0.9-m/t2ka	1.5
1997-06-18	50617.44	0.9-m/t2ka	1.4
1997-07-23	50652.32	0.9-m/t2ka	1.6

NOTE—Only the first three lines of Table 2 are shown here. It is published in its entirety in machine-readable format.

**Figure 2.** The number of epochs per year.

between observations is given in Figure 3, while the distribution of seeing values are plotted in Figure 4.

**Table 3.** Locations of New Novae

Name (M31N)	RA (J2000)	Dec (J2000)	$\Delta\alpha^a$ (")	$\Delta\delta^a$ (")
1995-09h	00:43:02.61	41:18:41.8	274.2	154.3
1997-06f	00:42:18.03	41:21:53.5	-394.5	346.0
1997-06g	00:42:44.78	41:16:48.2	6.7	40.7
1999-01e	00:42:44.38	41:16:16.1	0.8	8.6
1999-06c	00:42:38.60	41:14:19.2	-86.0	-108.3
1999-06d	00:42:39.32	41:16:11.3	-75.2	3.8
1999-07c	00:42:44.04	41:17:05.6	-4.3	58.1
1999-12f	00:43:06.37	41:30:14.0	330.6	846.5
1999-12g	00:41:37.15	41:05:51.2	-1007.7	-616.3
2001-11b	00:41:49.49	41:04:04.0	-822.6	-723.5
2002-06a	00:42:22.52	41:09:48.5	-327.2	-379.0
2002-06b	00:41:56.16	41:08:31.3	-722.5	-456.2
2002-06c	00:42:50.91	41:24:13.6	98.7	486.1
2002-08c	00:42:56.23	41:22:21.9	178.5	374.4
2002-09a	00:44:33.24	41:36:07.5	1633.7	1200.0
2002-09b	00:41:58.12	41:02:13.4	-693.1	-834.1
2002-11a	00:41:57.83	41:08:46.3	-697.5	-441.2
2003-06e	00:42:43.93	41:15:33.9	-6.0	-33.6
2003-08d	00:44:36.50	41:33:50.4	1682.5	1062.9
2003-08e	00:43:55.98	41:36:33.2	1074.8	1225.7
2003-10d	00:43:08.85	41:03:43.4	367.8	-744.1
2004-01c	00:42:46.21	41:05:38.2	28.2	-629.3
2004-06d	00:42:44.75	41:16:35.5	6.3	28.0
2004-06e	00:42:10.33	41:09:50.6	-510.0	-376.9
2004-06f	00:42:44.79	41:16:35.4	6.9	27.9
2005-11a	00:42:46.52	41:15:33.9	32.8	-33.6
2006-11d	00:43:05.61	41:01:29.8	319.2	-877.7
2006-11e	00:42:06.41	40:56:58.4	-568.8	-1149.1
2006-11f	00:41:56.88	40:58:43.9	-711.7	-1043.6
2007-06c	00:42:38.44	41:17:22.2	-88.3	74.7
2008-12c	00:42:43.95	41:16:59.1	-5.7	51.6
2008-12d	00:42:33.17	41:15:56.4	-167.4	-11.1
2011-09c	00:42:51.32	41:20:41.6	104.8	274.1
2011-09d	00:44:05.96	41:26:50.0	1224.4	642.5
2014-08a	00:43:47.72	41:33:13.2	950.8	1025.7
2014-08b	00:43:56.63	41:15:16.8	1084.5	-50.7
2015-11d	00:42:43.89	41:16:01.9	-6.6	-5.6
2016-10e	00:42:47.60	41:10:24.8	49.0	-342.7
2016-10f	00:42:34.37	41:15:52.6	-149.4	-14.9
2016-10g	00:42:23.67	41:12:05.6	-309.9	-241.9

NOTE—Only the 40 previously unreported novae are shown here. The astrometry for all 262 novae detected in this survey is published in its entirety in machine-readable format.

<sup>a</sup>Offset from the nucleus of M31.

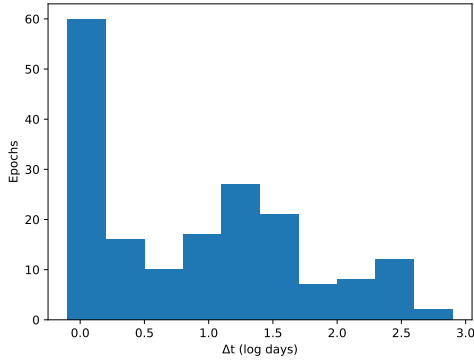


**Figure 3.** The distribution of time between epochs, in units of  $\log_{10}$  days.

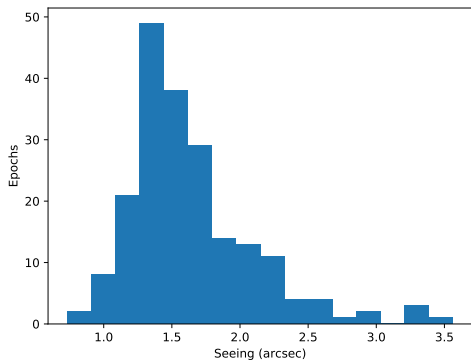


**Figure 4.** The distribution of seeing values.

The data were reduced with IRAF in the standard manner. The world coordinate system (WCS) was determined via stars from the USNO-B1.0 catalog (Monet et al. 2003) with a global solution RMS of better than  $0''.6$  in all cases. This is assumed as the accuracy for all measured positions. To remove geometric distortions and to allow for the images to be aligned, all of the images were projected to a common WCS and plate scale of  $0''.43 \text{ pixel}^{-1}$ , the plate scale of 0.9-m/MOSA. This scale was chosen so as to not degrade the stellar PSFs for most of the images. Data obtained with 4-m/MOSA had a smaller inherent plate scale and often better seeing, occasionally creating undersampled PSFs when rescaled. The original data were checked whenever the authenticity of a nova was in question. Because 0.9-m/MOSA also had the largest field of view ( $59' \times 59'$ ), data obtained with other camera and telescope configurations were scaled, aligned, and inset into larger blank images of this size so that epochs could be easily compared.

### 2.1. Nova Search Strategy

While automated searches for novae in M31 have made significant gains (e.g., Soraisam et al. 2017), searching

for novae in M31 is an ideal project for students because it is a relatively simple task that is well suited to human physiology, as our brains have evolved to detect subtle changes in complex environments. Over the two decades of the survey, each epoch was examined by hundreds of students as a blind study. Final confirmation of candidates was completed by the PIs.

Images were searched for novae with the following strategy: The 42 images taken with 0.9-m/MOSA were used to create a median image. Each epoch of observations was then divided by this median image, producing a “difference” image wherein stars and galactic structure largely canceled and novae appeared more prominently. This allowed the images to be searched in a uniform manner despite the tremendous differences in brightness between the core and outer parts of M31. Once a nova candidate was identified,  $100 \times 100$  pixel “cutouts” of that region were extracted from all 180 epochs to determine not only the veracity of the detection but its long-term behavior. Long-period variables could then be excluded. The positions of all nova candidates were compared with their locations on a deep 4-m image to see if any stellar objects were coincident.

### 2.2. Photometry

Aperture photometry was performed using the IRAF APPHOT package. To improve the photometry of novae within the bulge, the background light of M31 was fitted and subtracted with the IRAF IMSURFIT task. Tests indicated that removal of the background did not degrade the accuracy of photometric measurements for standard stars.

The 74  $H\alpha$  standard stars given in Ciardullo et al. (1987) were used to calibrate each epoch. Standards that deviated more than  $3\sigma$  were clipped, typically 1 to 5 stars per epoch. For the epochs obtained with the 1.3-m and 2.1-m telescopes, only 10-20 standards were in the FOV. For most epochs the standard star calibration is internally consistent to  $\sim 0.05$  mag.

The photometric calibration obtained from the Ciardullo et al. (1987) standards was compared to that determined by Massey et al. (2007) for the LGS fields. The Ciardullo et al. observations were obtained with a  $75\text{\AA}$  FWHM  $H\alpha$  filter, whereas the Massey et al. data, as well as ours, were obtained with  $50\text{\AA}$  FWHM  $H\alpha$  filters. To precisely compare the two we would need to know the full transmission profile for all of the filters; however, the two calibrations are consistent if the  $75\text{\AA}$ -wide filter allows about 30% more light to pass. For consistency with other work we use the Ciardullo et al. values.

Aperture photometry was completed for all nova candidates detected in our survey. For each nova a  $5\sigma$  detection upper limit was also calculated at the location of the nova in the epoch directly before first detection and in the epoch after it was last detected. Photometric measurements, as well as detection upper limits, are given in Table 4.

**Table 4.** Photometry for all Novae

Name	Date	Mag	Err
(M31N)	(MJD)	(H $\alpha$ )	
1994-09a	49963.26	18.68	$\pm 0.07$
1994-09a	50617.44	> 21.0	
1995-07a	49963.26	16.70	$\pm 0.03$

NOTE—Only the first three lines of Table 4 are shown here. It is published in its entirety in machine-readable format.

### 3. NOVA RATE IN OUR SURVEYED REGIONS

Of our observations only data obtained with two telescopes, the KPNO/WIYN 0.9-m and the KPNO 4-m, provide sufficient depth and temporal coverage to allow the spatial distribution and nova rate of M31 to be reliably determined. A spatially complete sample was defined of 203 novae detected by the 0.9-m telescope within a  $20' \times 20'$  field centered on the nucleus of M31. An additional 50 novae are part of a separate spatially complete sample discovered with the 4-m telescope within a  $36' \times 36'$  field centered on the nucleus. These surveys, which we will henceforth refer to as survey A and survey B respectively, have been analyzed separately and therefore provide two independent estimates of M31’s nova rate.

For both surveys, a determination of the nova rate in M31 depends on the intrinsic properties of the M31 nova population (i.e., their peak magnitudes, rates of decline, and whether these properties vary as a function of spatial position within the galaxy) and on the characteristics of the surveys themselves (i.e., the dates of observation, the survey’s effective limiting magnitude, and the number of novae discovered during the course of the survey). Of these parameters, only the dates of observation and the number of novae discovered are known with certainty. The photometric properties of the M31 nova population (what we will refer to as the instantaneous nova luminosity function), and the effective limiting magnitude of the survey (i.e., the completeness of the survey to a given apparent magnitude) are quantities that must either be assumed or estimated. The former is independent of the specifics of the survey, and will be the same for both surveys, while the latter must be determined for each survey separately. We explore each of these important considerations further below.

#### 3.1. The M31 Nova Luminosity Function

The intrinsic photometric (light curve) properties of the M31 nova population are not known a priori, and

must be estimated using existing nova H $\alpha$  light curves. Our best option to characterize the M31 nova luminosity function is to take the observed light curves of novae from this paper, augmented with similar observations from previous surveys (Ciardullo et al. 1987; Shafter & Irby 2001; Neill & Shara 2004). A potential drawback to this approach is that the existing observations of M31 nova light curves may suffer from observational selection biases. For example, a population of unusually faint and rapidly evolving novae, if it exists, could be under-represented in our observed light curve sample. Fortunately, we see no evidence for such a putative population of faint and fast novae in our extensive data set. Finally, given that there is no compelling evidence to the contrary, we have assumed that the nova properties do not vary significantly with spatial position within M31.

Not all of the novae discovered in our surveys have sufficient temporal coverage to allow reliable light curve parameters (i.e., peak magnitudes and fade rates) to be determined. In particular, the discovery magnitude will usually underestimate the peak brightness of the nova unless maximum light is well covered by the observations, and this is typically not the case. In order to mitigate the discrepancy between the observed peak and the true peak magnitude, we have restricted our light curve sample to those novae where either maximum light can be constrained by observations made on the rise to peak, or in cases where a previous observation (or null detection) was available up to a month before the observed maximum. In the latter case we have estimated peak magnitude by extrapolating the best fit of the declining branch of the light curve backwards to the midpoint between the time of the observed maximum and that of the previous measurement or non-detection.

After applying these selection criteria to our overall nova sample, we were left with 30 novae with sufficiently well-sampled light curves suitable for use in our M31 nova rate simulations (see Figure 5 for their light curves and Table 5 for their calculated parameters). In addition to these novae, Table 5 also lists 13 novae from the literature with measured peak H $\alpha$  magnitudes and fade rates. In Figure 6 we show the absolute H $\alpha$  magnitudes for all 43 novae plotted as a function of the fade rate, as parameterized by the log of the time in days it takes for a nova to fade by two magnitudes. As expected based on the work of Ciardullo et al. (1987), there is no compelling evidence for a maximum magnitude, rate-of-decline (MMRD) relationship for the H $\alpha$  light curves.

### Fig. Set 5. Light curves for novae used in the Monte Carlo simulations

#### 3.2. The Effective Limiting Magnitude of the Survey

A determination of the completeness of survey A (0.9-m) and survey B (4-m) is central to a determination of the galaxy’s nova rate. In addition to the characteristics

**Table 5.** Light Curve Parameters

Nova					$f_{\text{H}\alpha}$	$\sigma_{f_{\text{H}\alpha}}$	$t_2(\text{H}\alpha)$	$\sigma_{t_2}$		
(M31N)	$m_{\text{H}\alpha}$	$\sigma_m$	$M_{\text{H}\alpha}$	$\sigma_M$	(mag d <sup>-1</sup> )	(mag d <sup>-1</sup> )	(d)	(d)	log( $t_2$ )	Ref <sup>a</sup>
1997-08b	16.42	0.09	-8.09	0.10	0.0063	0.0003	318.0	15.3	2.50	1
1998-07d	15.81	0.11	-8.71	0.12	0.0098	0.0007	204.8	14.0	2.31	1
1998-08a	16.05	0.16	-8.46	0.16	0.0086	0.0009	232.7	24.6	2.37	1
1998-08b	15.41	0.29	-9.10	0.30	0.0245	0.0038	81.6	12.6	1.91	1
2000-10a	16.64	0.02	-7.87	0.05	0.0321	0.0003	62.2	0.6	1.79	1
2002-08a	15.60	0.10	-8.91	0.11	0.0174	0.0018	115.1	12.0	2.06	1
2003-06b	16.05	0.11	-8.46	0.12	0.0220	0.0015	91.0	6.1	1.96	1
2003-06c	15.12	0.26	-9.40	0.27	0.0262	0.0034	76.2	9.8	1.88	1
2003-06d	15.95	0.16	-8.57	0.16	0.0224	0.0021	89.3	8.4	1.95	1
2003-07b	16.86	0.08	-7.65	0.09	0.0295	0.0016	67.8	3.8	1.83	1
2003-08a	16.69	0.13	-7.83	0.14	0.0210	0.0041	95.5	18.5	1.98	1
2003-08b	15.58	0.07	-8.94	0.09	0.0230	0.0009	87.0	3.2	1.94	1
2003-09a	15.88	0.09	-8.63	0.11	0.0311	0.0014	64.4	2.8	1.81	1
2003-09b	16.08	0.26	-8.43	0.27	0.0184	0.0046	108.6	27.2	2.04	1
2003-10c	15.77	0.01	-8.74	0.05	0.0219	0.0008	91.2	3.2	1.96	1
2003-11a	16.53	0.12	-7.98	0.13	0.0235	0.0021	85.1	7.6	1.93	1
2003-11b	15.26	0.11	-9.25	0.12	0.0368	0.0029	54.3	4.2	1.73	1
2003-12a	16.31	0.06	-8.20	0.08	0.0144	0.0006	139.1	5.3	2.14	1
2003-12b	16.20	0.04	-8.32	0.06	0.0182	0.0016	109.7	9.4	2.04	1
2003-12c	15.30	0.18	-9.22	0.19	0.1282	0.0080	15.6	1.0	1.19	1
2004-01a	15.23	0.07	-9.29	0.09	0.0134	0.0003	148.8	3.8	2.17	1
2004-10a	15.79	0.11	-8.72	0.12	0.0441	0.0054	45.3	5.5	1.66	1
2005-10b	15.77	0.10	-8.75	0.11	0.0238	0.0018	84.2	6.2	1.93	1
2009-08e	16.08	0.05	-8.43	0.07	0.0108	0.0010	184.5	16.5	2.27	1
2009-10b	15.60	0.12	-8.92	0.13	0.0084	0.0004	237.8	12.2	2.38	1
2009-11b	16.66	0.09	-7.85	0.10	0.0247	0.0027	81.1	8.9	1.91	1
2009-11e	15.84	0.10	-8.67	0.11	0.0314	0.0037	63.7	7.5	1.80	1
2010-06a	17.15	0.11	-7.36	0.12	0.0218	0.0022	91.7	9.2	1.96	1
2010-10a	16.35	0.18	-8.17	0.19	0.0258	0.0035	77.6	10.5	1.89	1
2010-10d	16.19	0.36	-8.33	0.36	0.0308	0.0094	64.8	19.7	1.81	1
1982-09e	15.42	...	-9.09	...	0.0800	...	25.0	...	1.40	2
1985-10b	14.76	...	-9.75	...	0.0290	...	69.0	...	1.84	2
1986-09a	15.68	...	-8.83	...	0.0130	...	153.8	...	2.19	2
1992-12a	16.20	...	-8.31	...	0.0070	...	285.7	...	2.46	3
1995-08d	18.40	...	-6.11	...	0.0460	...	43.5	...	1.64	3
1995-08e	16.10	...	-8.41	...	0.0150	...	133.3	...	2.12	3
1995-11d	16.60	...	-7.91	...	0.0090	...	222.2	...	2.35	3
2003-01b <sup>b</sup>	15.60 <sup>c</sup>	...	-8.91	...	0.0210	...	95.2	...	1.98	4
2003-02a <sup>b</sup>	14.90 <sup>c</sup>	...	-9.61	...	0.1290	...	15.5	...	1.19	4
2003-02b <sup>b</sup>	15.80 <sup>c</sup>	...	-8.71	...	0.0310	...	64.5	...	1.81	4
2003-03a <sup>b</sup>	14.60 <sup>c</sup>	...	-9.91	...	0.0780	...	25.6	...	1.41	4
2003-05d <sup>b</sup>	15.10 <sup>c</sup>	...	-9.41	...	0.0360	...	55.6	...	1.75	4
2003-06a <sup>b</sup>	15.50 <sup>c</sup>	...	-9.01	...	0.0870	...	23.0	...	1.36	4

<sup>a</sup>(1) This work; (2) Ciardullo et al. (1990); (3) Shafter & Irby (2001); (4) Neill & Shara (2004)<sup>b</sup>M81N<sup>c</sup>Corrected for H $\alpha$  bandpass (30Å vs 75Å) and  $\Delta m$ , adopting  $\mu_o(\text{M81}) = 27.8$  (Freedman et al. 2001).

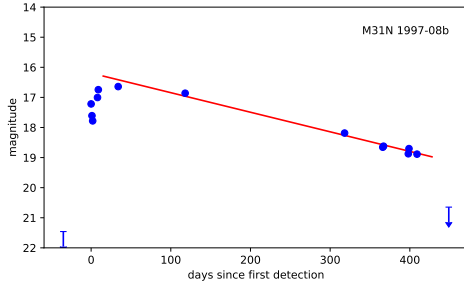


**Figure 5.** The light curve for nova M31N 1997-08b, one of 30 novae used in the Monte Carlo simulations. The complete figure set of 30 plots is available in the online journal. The vertical axis shows the  $H\alpha$  magnitude. The horizontal axis shows the number of days since first detection. Upper-limits on detection are also plotted for prior observations within 31 days of the first detection, as well as for observations obtained within 100 days of the last detection. The red line shows the linear best fit during the decline. In some figures a red plus sign marks the estimated location of peak magnitude, as extrapolated from the rise and decay slopes.

of the surveys themselves (e.g., the telescope apertures, the integration times, and the plate scales), the overall completeness to a given apparent magnitude  $C(m)$  will be strongly dependent on the brightness of, and variation in, the background light of the host galaxy. Since the galaxy background light is non-uniform across the survey images, the simplest and most effective approach to estimating the completeness of extragalactic nova surveys is to conduct artificial star (nova) tests. Thus, following our earlier work (e.g., see [Shafter et al. 2021](#), and references therein), we have conducted artificial nova tests on representative images from both survey A and survey B (hereafter the fiducial images).

In performing the simulations, one must decide how to treat the spatial distribution of the artificial novae. Here, as in previous studies, we have chosen to proceed under the assumption that the spatial distribution of the artificial novae follows the background light of the galaxy. Such an assumption might be questionable if the nova rate was a strong function of stellar population, for example. However, since our central field is dominated by light from a single population (M31’s bulge), we consider our approach to be justified.

Artificial novae with PSFs that matched the stars in our fiducial images were generated using tasks in the IRAF DAOPHOT package. The fiducial images were then seeded with 100 artificial novae with random apparent magnitudes lying within each of eight 0.5 mag wide bins using the routine `addstar`. For each of the magnitude bins, the artificial novae were distributed at random locations within each image, but with a spatial density that was constrained to follow the surface brightness of M31. Artificial novae were then recovered using

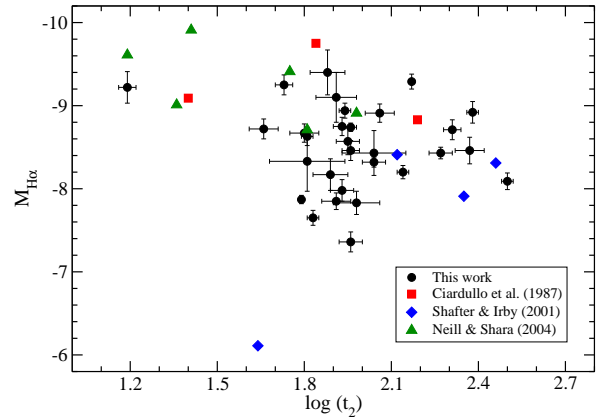


**Figure 6.** The peak  $H\alpha$  absolute magnitudes for the novae used in our Monte Carlo analysis plotted as a function of the fade rate as measured by  $\log(t_2)$ . There is no evidence for an  $H\alpha$  MMRD relation as first demonstrated by [Ciardullo et al. \(1987\)](#).

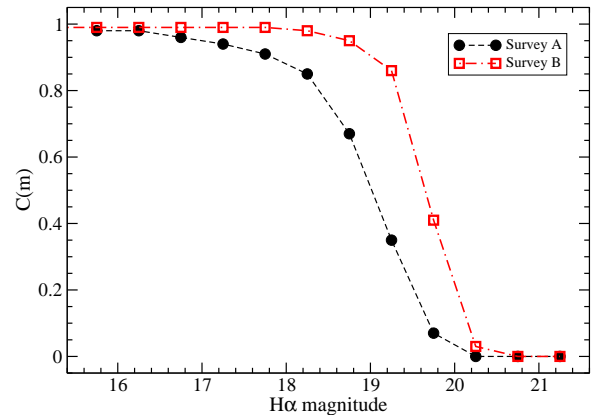


**Figure 7.** The completeness of surveys A and B as a function of apparent  $H\alpha$  magnitude as determined from the artificial nova tests.

the same procedures that were employed in identifying novae in our survey images.

The fraction of artificial novae recovered in our searches in each magnitude bin yielded the completeness functions  $C(m)$  shown in Figure 7. In cases where the different epochs of observation were obtained under different conditions (e.g., different telescopes, integration times, etc.), this completeness function can be generalized to any epoch,  $i$ , of observation by applying a shift,  $\Delta m_i (= m_{\text{lim},0} - m_{\text{lim},i})$ . Thus, for any epoch,  $i$ , we have  $C_i(m) = C(m + \Delta m_i)$ . In the case of our M31

nova surveys, the limiting magnitudes of the individual images were sufficiently similar that we were able to use the same completeness function for all epochs from a given survey.

### 3.3. Numerical Simulations

Armed with an estimate of the instantaneous nova luminosity function and the completeness functions  $C(m)$  for surveys A and B, we are now in a position to estimate the nova rate  $R$  in our two surveyed regions of M31. Following the procedure adopted in our previous extragalactic nova studies (e.g., Shafter et al. 2021; Franck et al. 2012; Güth et al. 2010; Coelho et al. 2008; Williams & Shafter 2004), we have performed numerical experiments to estimate the intrinsic nova rate  $R$  that will most likely produce the number of M31 novae that we have detected during the course of our surveys.

We begin by producing trial novae erupting at random times throughout the time span covered by a given survey. Each simulated nova was given the parameters of one of the 30 novae selected at random. Again it is worth noting that these parameters are based on novae discovered in our survey, supplemented by light curves measured in previous M31 nova studies (Ciardullo et al. 1990; Shafter & Irby 2001). They are therefore subject to observational selection biases and may not necessarily represent the full range of nova properties. Ideally, we would like to use light curve parameters specific to the full population of M31 novae, but such an unbiased sample does not exist. Instead, we used the M31 light curve parameters from our observations given in Table 5, augmented with additional H $\alpha$  light curve parameters from the nova light curves observed by Ciardullo et al. (1990), Shafter & Irby (2001), and Neill & Shara (2004).

The number of novae expected to be discovered during the course of a given survey as a function of the assumed nova rate  $N_{\text{obs}}(R)$  can then be computed by convolving the simulated apparent magnitude distribution for a given epoch of observation  $n_i(m, R)$  with the completeness function  $C(m)$  and then summing over all epochs of observation:

$$N_{\text{obs}}(R) = \sum_i \sum_m C(m) n_i(m, R). \quad (1)$$

The best estimate of the intrinsic nova rate  $R$  in the regions covered by each survey, and their associated uncertainties is determined by comparing the number of novae found in a given survey  $n_{\text{obs}}$  with the number of novae predicted by equation (1). We explored trial nova rates ranging from  $R = 1$  to 50 novae per year, repeating the numerical simulation a total of  $10^5$  times for each trial value of  $R$ . The number of matches  $M(R)$  between the predicted number of observable novae  $N_{\text{obs}}(R)$  and the actual number of novae discovered in each of our surveys,  $n_{\text{obs}} = 203$  for survey A and  $n_{\text{obs}} = 50$  in survey B, was recorded for each trial value of  $R$ . The values of  $M(R)$  were then normalized by the total number

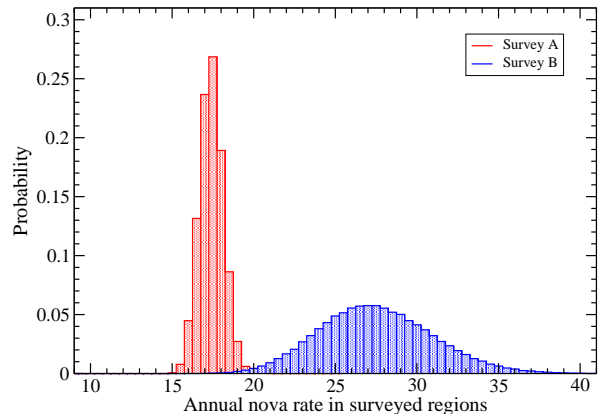


**Figure 8.** The results of the numerical nova rate simulation for the  $20' \times 20'$  and the  $36' \times 36'$  surveyed regions of surveys A and B. The most probable nova rates in the surveyed regions are  $R_A = 17.5_{-0.4}^{+0.9}$  and  $R_B = 27.0_{-3.0}^{+3.8}$  per year, respectively.

of matches for all  $R$  to give the probability distribution functions,  $P(R) = M(R) / \sum_R M(R)$  shown in Figure 8. The most probable nova rate in the portion of the galaxy covered by our survey images is  $R_A = 17.5_{-0.4}^{+0.9} \text{ yr}^{-1}$  and  $R_B = 27.0_{-3.0}^{+3.8} \text{ yr}^{-1}$  for surveys A and B, respectively. The  $1\sigma$  error range for the probability distributions were computed by assuming they can be approximated as bi-Gaussian functions.

## 4. THE NOVA SPATIAL DISTRIBUTION

The spatial distributions of the 203 novae in survey A and the 50 novae found in survey B are shown superimposed on (negative) DSS2 red images of M31 in Figures 9 and 10, respectively. In both cases the surface density of novae appears to generally follow the background light of M31, increasing markedly toward the center of the galaxy.

### 4.1. Comparison with the Background light

A quantitative assessment of how well the nova density follows the surface brightness of the galaxy can be achieved by comparing their cumulative distributions as a function of galactocentric radius (i.e., the semimajor axis of the elliptical isophote passing through the position of a given nova). These cumulative distributions of novae and the background  $B$  and  $R$ -band light from the surface photometry of de Vaucouleurs (1958) and Kent (1987) are shown in Figures 11 and 12 for surveys A and B, respectively.

As expected, the nova distributions follow the background light of the galaxy more closely at longer wavelengths (i.e., better in  $R$  compared to  $B$ ), and better for survey B with its larger field-of-view ( $36' \times 36'$ ) than for the smaller  $20' \times 20'$  field covered by survey A. This

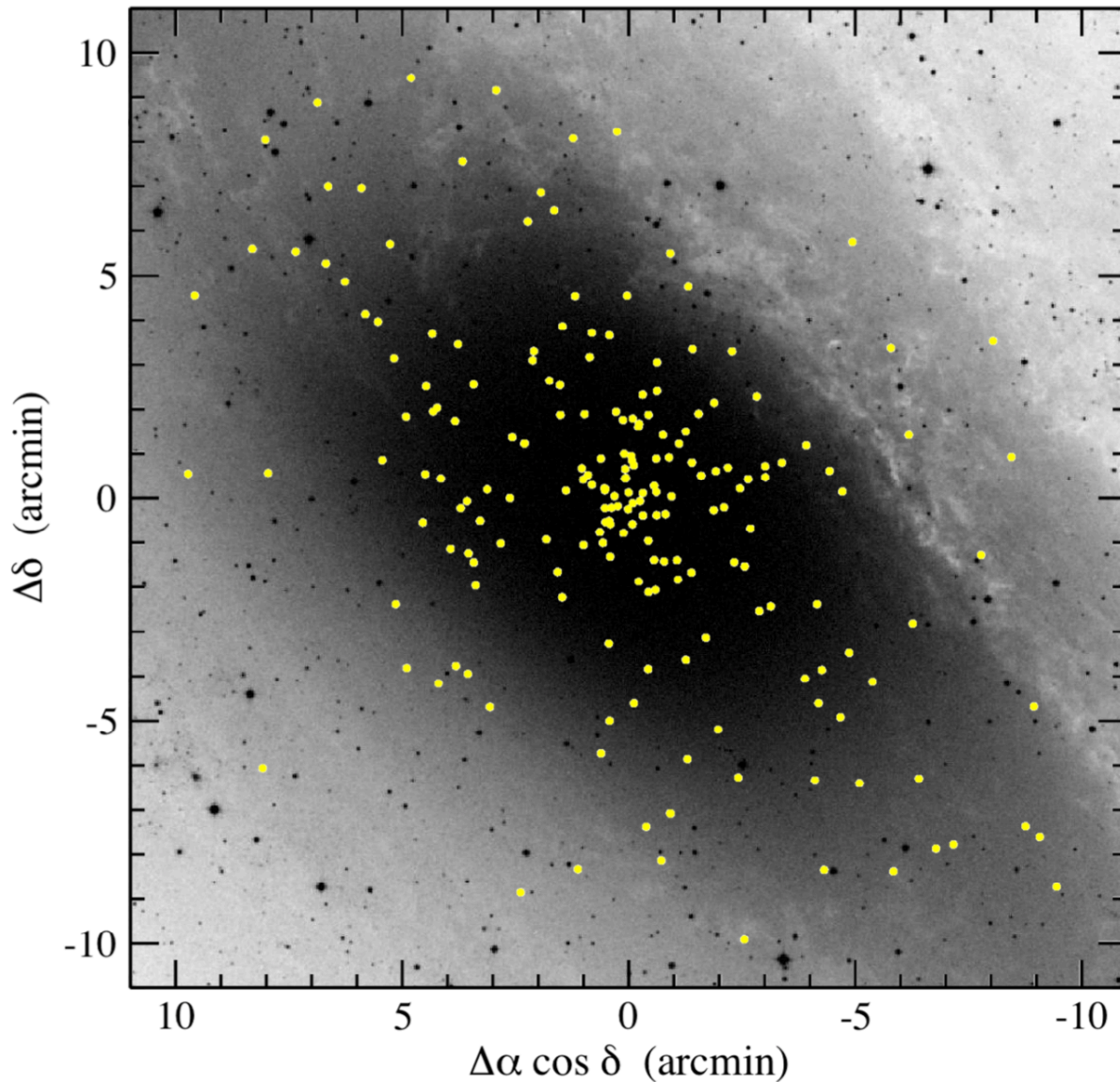


**Figure 9.** The spatial distribution of the 203 novae found within our  $20' \times 20'$  field of survey A, superimposed on a DSS2 red image of M31.

difference can be attributed to the fact that the portion of M31 covered in survey A is dominated by the galaxy’s bulge population. The bulge light, consisting mostly of lower mass Pop II stars is “redder” than the disk light, and traces the mass in stars more closely than does the  $B$ -band light, which is more affected by a smaller number of massive blue main-sequence stars associated with the galaxy’s disk population. In all cases, Kolmogorov-Smirnov (KS) tests show that the probabilities that the distributions are drawn from the same parent distribution are unlikely. The best fit, when the 50 novae from survey B is compared with the galaxy’s  $R$  band light, yields a KS statistic of just 0.1, indicating that the nova and light distributions differ with 90% confidence.

In order to explore whether the poor fit to the background light results from a nova density distribution that varies with stellar population, it is useful to compare the nova distribution with the galaxy’s bulge and disk light separately, as well as with different proportions of bulge and disk light.

#### 4.2. Bulge-Disk Separations

Optical surface photometry of M31 that can be used to separate the bulge and disk components of the galaxy’s light has been undertaken in several studies going back to the photographic work of [de Vaucouleurs \(1958\)](#). In recent years, infrared surface photometry made possible with 2MASS ([Jarrett et al. 2003](#)) and *Spitzer* ([Fazio et al. 2004](#)) has become available, which should better

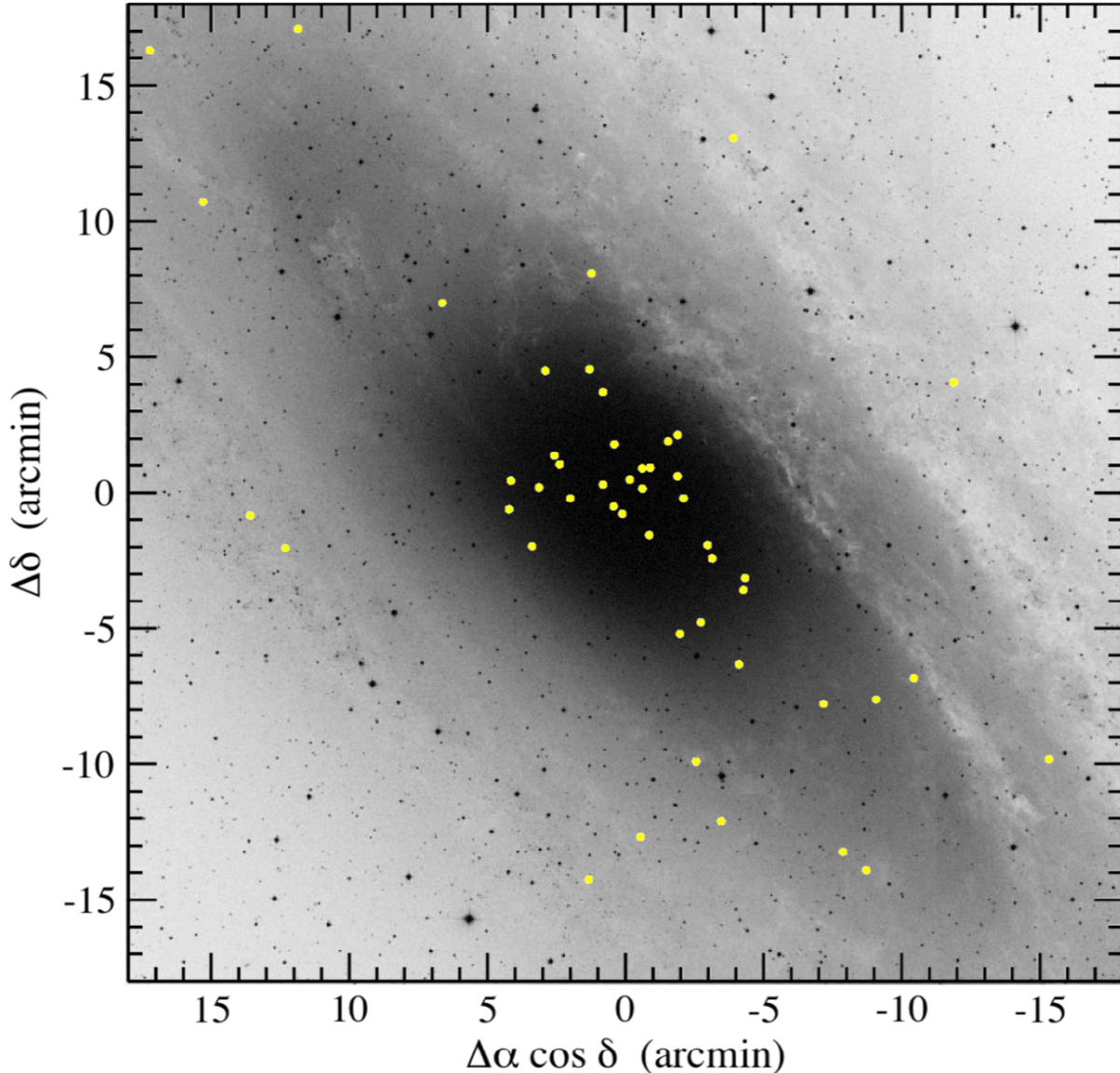


**Figure 10.** The spatial distribution of the 50 novae found within our  $36' \times 36'$  field of survey B, superimposed on a DSS2 red image of M31.

trace the mass of the galaxy. Armed with these data, an extensive set of M31 bulge-disk separations have been performed by Courteau et al. (2011) who modeled the infrared light with a Sersic bulge profile combined with an exponential disk component. These decompositions have been performed using multiple techniques, including non-linear least-squares and Markov Chain Monte-Carlo techniques on 1D radial light profiles from major and minor axis cuts, or on azimuthal averages. For the fitting of 2D images, they have adopted the GALFIT galaxy/point source fitting algorithm of Peng et al. (2002). As discussed by Courteau et al. (2011), the 2D GALFIT models are less affected by non-axisymmetric features like the galaxy’s spiral arms. So, for our pur-

poses, we have adopted their Model P decomposition of the M31 IRAC ( $3.6\mu$ ) bulge, disk, and total infrared light. We have explored other models, and found that the results of our analysis are not sensitive to the choice of model used in the bulge-disk decomposition.

Figure 13 shows the cumulative M31 nova distribution for the  $20' \times 20'$  region of survey A as compared with the cumulative (disk, bulge, and combined) light from model P of Courteau et al. (2011). As has been found in several previous M31 studies (e.g., Ciardullo et al. 1987; Capaccioli et al. 1989; Shafter & Irby 2001), when the bulge and disk light are considered separately, it is clear that the novae follow the galaxy’s bulge light consider-

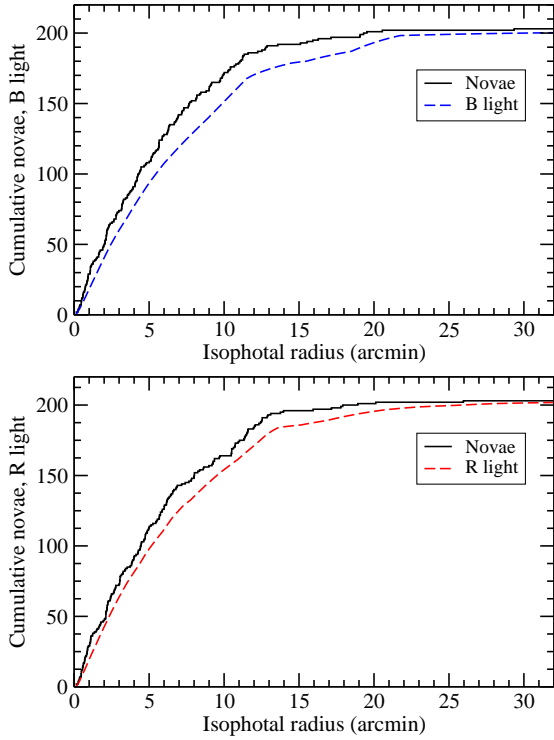


**Figure 11.** The cumulative nova density from survey A compared with the integrated background light of M31. Top panel: B light from [de Vaucouleurs (1958)]; Bottom panel: R light from Kent (1987). The likelihoods that the nova density match the background light are 0.57% and 5.5% for the *B* and *R* bands, respectively.

ably better than they do the disk light<sup>6</sup>. In the case of our survey A in particular, this is not surprising given that the light in the central  $20' \times 20'$  surveyed region is dominated by the bulge, which contains  $\sim 70\%$  of the enclosed light. However, a much better fit is achieved when the overall (bulge+disk) galaxy light is considered (lower left panel of Figure 13). Furthermore, the cumulative nova distribution follows  $3.6\mu$  galaxy light considerably better (KS=0.22) than it does the *B* and *R*-band light (KS=0.0057 and KS=0.055, respectively) as seen in Figures 11 and 12.

Figure 14 shows the cumulative nova and light distributions for the  $36' \times 36'$  region of survey B. As seen in survey A, the nova distribution follows the bulge light better than the disk light, but the larger coverage of survey B results in an even better fit of the cumulative nova distribution to the overall  $3.6\mu$  galaxy light (KS=0.26).

<sup>6</sup> See Hatano et al. (1997) for a different interpretation.

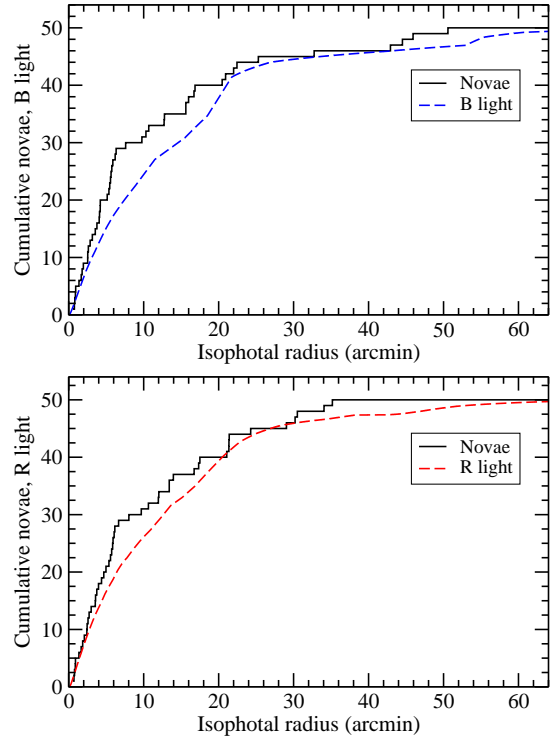


**Figure 12.** The cumulative nova density from survey B compared with the integrated background light of M31. Top panel: B light from [ref]; Bottom panel: R light from Kent (1987). The likelihoods that the nova density match the background light are 1.5% and 10%, for the *B* and *R*-bands, respectively.

Once again, the nova distribution follows the near infrared  $3.6\mu$  light much better than in the case of the *B* and *R*-band comparisons.

The apparent affinity of novae for M31's bulge population is consistent with the results of Shafter et al. (2011) who found that  $\sim 80\%$  of spectroscopically-confirmed M31 novae belong to the Fe II class (e.g., see Williams 1992). In studies of the Milky Way, Della Valle & Livio (1998) have shown that Fe II and He/N novae are associated primarily with the bulge and disk, respectively.

#### 4.2.1. Optimum Bulge-Disk Nova Densities

We can determine the optimum ratio of bulge and disk nova densities required to provide the best match to the overall galaxy light by performing a maximum likelihood analysis that compares the spatial positions of the novae with the bulge and disk light distributions, as originally described in Ciardullo et al. (1987). The observed spatial distribution of novae is compared with a theoretical distribution function where the probability

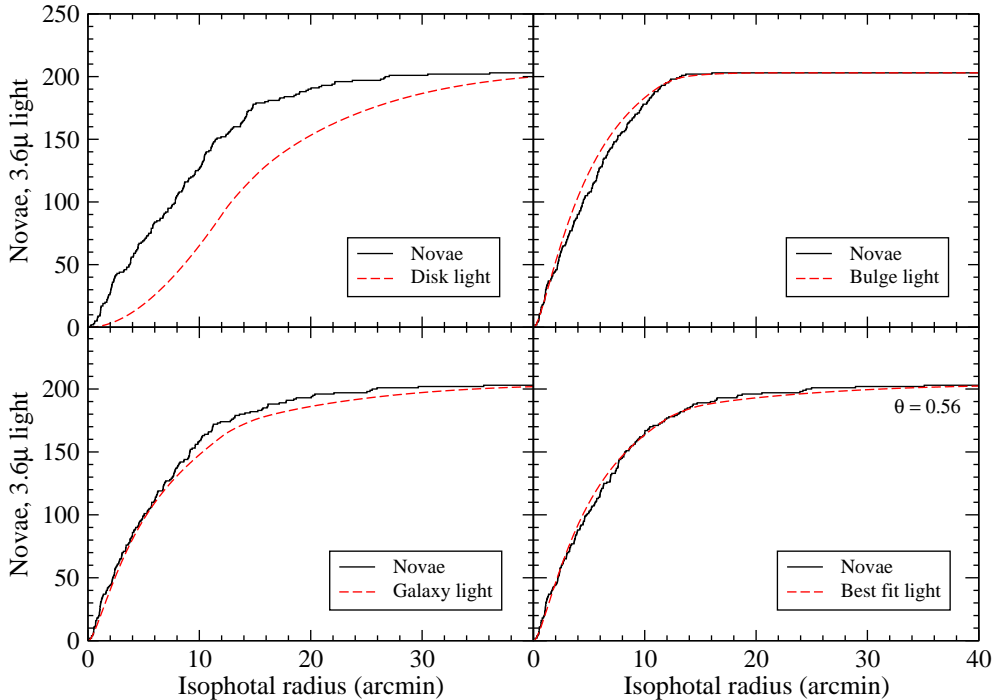


**Figure 13.** The cumulative distributions of novae within our  $20' \times 20'$  survey region compared with the cumulative distributions of M31 light from Model P of Courteau et al. (2011). The nova distribution is compared with the disk, bulge, total galaxy, and the best fit disk+bulge ( $\theta = 0.56$ ) light in the upper left, upper right, lower left and lower right panels, respectively, with corresponding KS values comparing the nova and light distributions of  $\sim 0, 0.053, 0.22,$  and  $0.74$ .

of a nova occurring at a given location in the galaxy depends both on the relative disk-to-bulge luminosity at that location and on an assumed ratio of disk and bulge nova rates, defined as  $\theta = \rho_{\text{disk}}/\rho_{\text{bulge}}$ . Specifically, the probability of a nova appearing at a position  $x$  in the galaxy is given by:

$$P(x, \theta) = \frac{L_{\text{bulge}}(x) + \theta L_{\text{disk}}(x)}{\sum_x [L_{\text{bulge}}(x) + \theta L_{\text{disk}}(x)]}, \quad (2)$$

where the relative luminosity of the disk to the bulge has been determined from the decomposition of the overall galaxy light as described earlier. The value of  $\theta$  is varied until the probability that the observed distribution is drawn from the theoretical distribution  $P(x, \theta)$  is maximized. In practice, this is accomplished by defining a merit function,

$$Q(\theta) = \sum_x \ln P(x, \theta), \quad (3)$$

and finding the value of  $\theta$  corresponding to its maximum.

The maximum-likelihood analysis is most accurate when applied to a large field containing significant bulge

and disk populations. In view of the limited spatial coverage of survey A, which is dominated by M31's bulge population, we have chosen to apply the maximum likelihood analysis to survey B given its significantly larger field-of-view that includes roughly equal proportions of bulge and disk light (51% bulge, 49% disk).

The result of our analysis applied to the bulge and disk surface brightness profiles given by Model P of Courteau et al. (2011) is shown in Figure 15. The optimum fit corresponds to  $\theta_{\text{max}} = 0.56^{+0.23}_{-0.17}$  (probable errors) implying a somewhat stronger association of novae with M31's bulge component. However the resulting distribution is quite broad, suggesting that  $\theta_{\text{max}}$  is relatively poorly constrained. Overall, the analysis is consistent with the conclusion that novae are associated with both the bulge and disk populations of M31, with rates that are not strongly dependent on stellar population.

The nova density distributions from both surveys A and B are compared with the optimum combined light distributions based on  $\theta = 0.56$  in the lower right panels of Figures 13 and 14. For both surveys the fit is remarkably good.

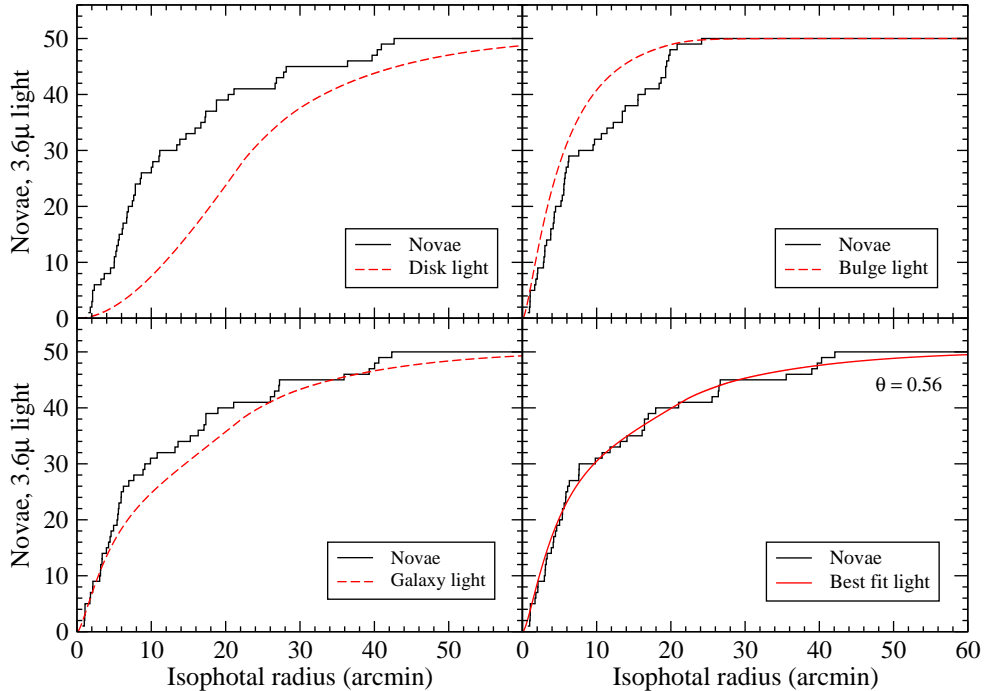


**Figure 14.** The cumulative distributions of novae within our  $36' \times 36'$  survey region of the 4-m mosaic images compared with the cumulative distribution of M31 light from Model P of Courteau et al. (2011). As with Figure 13, the nova distribution is compared with the disk, bulge, total galaxy, and the best fit disk+bulge ( $\theta = 0.56$ ) light in the upper left, upper right, lower left and lower right panels, respectively, with corresponding KS values comparing the nova and light distributions of  $\sim 0$ , 0.034, 0.26, and 0.90.

### 5. THE GLOBAL M31 NOVA RATE

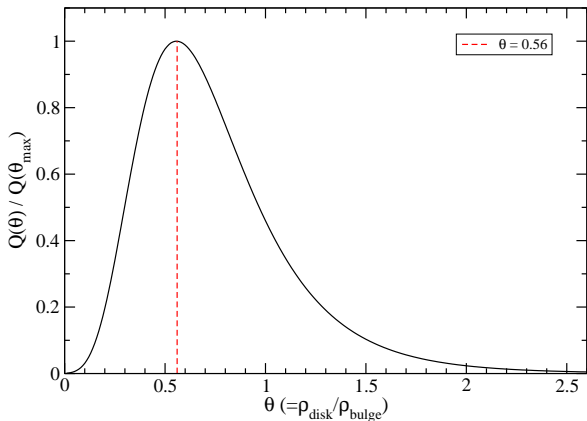
In order to determine the global nova rate for M31, our estimate of the rate in the surveyed regions must be extrapolated to the entire galaxy. In performing such extrapolations, it has been traditionally assumed that  $\theta = 1$ , i.e., that the luminosity-specific nova rate is constant across the galaxy’s bulge and disk populations. This is the only extrapolation possible without modeling the bulge and disk light separately. Under this assumption, the extrapolation is simply based on the fraction of the galaxy’s integrated light in waveband  $\lambda$  contained within the surveyed region,  $f_S(\lambda)$ . To provide the best proxy for the fraction of the mass in stars contained within the surveyed region, longer wavebands ( $R$ -band through the near infrared) are usually preferred.

Table 6 shows the values of  $f_S(\lambda)$  and the subsequent global M31 nova rates based on extrapolations using the light in the bandpasses we have considered (B, R, and the IRAC  $3.6\mu$  bands). With the exception of the  $\theta = 0.56$  case, where a probable error has been computed, an error of 10% in the values of  $f_S(\lambda)$  has been

assumed when propagating errors from the nova rates in the surveyed regions to the final extrapolated M31 nova rates. In the case of the IRAC data, we have used bulge-disk separations given by Model P from Courteau et al. (2011) to enable extrapolations based on nova densities that vary with stellar population (i.e., values of  $\theta$  that differ from unity).

As discussed earlier, extrapolations based on red or infrared photometry are preferred as they are believed to trace the underlying mass in stars, and, as we have seen, the fits of the cumulative nova density distribution to the background light improves with increasing wavelength. Thus, we prefer to use the IRAC  $3.6\mu$  photometry to extrapolate the nova rate in our surveyed regions to the entire galaxy.

The question of whether to allow the specific nova rate to vary between the bulge and disk populations is less clear. On the one hand, the measured luminosity-specific nova rates of galaxies do not appear to vary systematically across a wide range of Hubble types (e.g., see Shafter et al. 2014). Although some late-type galaxies,



**Figure 15.** The results of our maximum likelihood analysis plotted as a function of the assumed disk-to-bulge nova density,  $\theta$ . The relative bulge and disk surface brightness is based on model P of Courteau et al. (2011). The analysis has been applied to the wider field 4-m survey (survey B), because its more extensive coverage ( $36' \times 36'$ ) provides a nearly equal balance between M31’s bulge and disk populations. The most probable value of  $\theta_{\max} = 0.56_{-0.17}^{+0.23}$ .

such as the Large and Small Magellanic Clouds and the nearly bulge-less spiral M33, appear to have somewhat larger than average luminosity-specific nova rates (e.g., see della Valle et al. 1994), the value for the early-type giant elliptical galaxy M87 also appears to be elevated (Shara et al. 2016; Shafter et al. 2017). Taken together, these observations suggest that the nova rate across M31 may not be particularly sensitive to the galaxy’s changing bulge and disk populations.

On the other hand, however, multiple studies of the spatial distribution of novae in M31 have found that the nova distribution tracks the bulge component of the galaxy as well, or in some cases better, than the overall background light (e.g., see Ciardullo et al. 1987; Shafter & Irby 2001; Darnley et al. 2006; Kaur 2016) suggesting that the specific nova rates are in fact affected by stellar population. Given the considerably improved fits to the background light that are achieved when allowing for differing bulge and disk nova densities, we have chosen to extrapolate the nova rate in our surveyed regions to the entire galaxy using our optimum  $\theta = 0.56$  light distribution. Taking the mean<sup>7</sup> of our rates for surveys A and B from Table 6 gives a best estimate for the global M31 nova rate of  $R_{\text{M31}} = 40_{-4}^{+5} \text{ yr}^{-1}$ . We note that the quoted (formal) uncertainty is based on

<sup>7</sup> We have chosen not to apply any weighting. Even though survey A contains more novae, survey B covers a significantly larger portion of the galaxy.

the propagation of essentially Poisson errors from our numerical simulations, and therefore does not fully take into account possible systematic errors in our analysis (e.g., in properly assessing the effective limiting magnitude of our survey). Thus, these errors likely represent a lower limit to the true uncertainty in the derived nova rate.

### 5.1. The Luminosity-Specific Nova Rate

To enable a comparison of the nova rate in M31 with other galaxies, it is necessary to normalize the rate to an intrinsic property of the galaxy. Ideally, one would like to standardize the rate to the total mass in stars. However, given that the stellar mass cannot be measured directly, it has been standard practice to normalize extragalactic nova rates to the infrared (typically the  $K$ -band) luminosity of the galaxy, which is thought to trace the underlying stellar mass quite well.

In order to compute the integrated  $K$ -band luminosity of M31 we have chosen to adopt an apparent  $K$ -band magnitude of  $K_{\text{M31}} = -0.04$  based on the analysis of *Spitzer* IRAC data presented in Barmby et al. (2006). Adopting a distance modulus for M31,  $\mu_o(\text{M31}) = 24.38 \pm 0.05$  (Freedman et al. 2001), along with an absolute  $K$ -band magnitude for the sun of  $M_{K,\odot} = 3.27$  (Willmer 2018), yields an integrated  $K$ -band luminosity for M31 of  $L_K(\text{M31}) = 1.2 \times 10^{11} L_{\odot,K}$ . This value is in excellent agreement with a value of  $L_{3.6\mu}(\text{M31}) = 1.17 \times 10^{11} L_{\odot,3.6\mu}$  quoted by Courteau et al. (2011) in their decomposition of M31’s IRAC light. The corresponding  $K$ -band luminosity-specific nova rates  $\nu_K$ , along with their estimated uncertainties, are given in the final column of Table 6.

In the case of our preferred IRAC  $\theta = 0.56$  extrapolation, we find an average  $K$ -band luminosity-specific nova rate based on our two surveys to be  $\nu_K = 3.3 \pm 0.4$  novae per year per  $10^{10}$  solar luminosities in the  $K$  band. This value is slightly higher, but not inconsistent with the mean for galaxies with measured nova rates,  $\nu_K = 2.25 \text{ yr}^{-1} [10^{10} L_{K,\odot}]^{-1}$ , found by Shafter et al. (2014).

## 6. DISCUSSION

The nova rate in M31 has been estimated many times going back to Hubble’s early work at Mount Wilson during the first three decades of the twentieth century. The results of key studies are summarized in Table 7. After beginning with estimates of order 30 per year from the pioneering photographic surveys of Hubble (1929), Arp (1956), and Rosino (e.g., see Capaccioli et al. 1989), it is interesting that measurements of the M31 nova rate have crept up in recent years, with a rate of  $65_{-15}^{+16} \text{ yr}^{-1}$

**Table 6.** M31 Nova Rate Estimates

Band	$\lambda_{\text{eff}}(\mu)$	$\theta (= \rho_d/\rho_b)$	$f_S(\lambda)$	$R_{\text{M31}}$ ( $\text{yr}^{-1}$ )	$\nu_K$ ( $\text{yr}^{-1} [10^{10} L_{\odot,K}]^{-1}$ )
Survey A: $R_A = 17.5^{+0.9}_{-0.4}$					
<i>B</i>	0.44	1.0	$0.34 \pm 0.02$	$52^{+5}_{-4}$	$4.3^{+0.5}_{-0.5}$
<i>R</i>	0.64	1.0	$0.37 \pm 0.03$	$48^{+4}_{-4}$	$4.0^{+0.5}_{-0.4}$
IRAC	3.6	1.0	$0.38 \pm 0.03$	$46^{+4}_{-3}$	$3.9^{+0.5}_{-0.4}$
IRAC	3.6	$0.56^{+0.23}_{-0.17}$	$0.48^{+0.07}_{-0.06}$	$37^{+6}_{-5}$	$3.0^{+0.5}_{-0.5}$
Survey B: $R_B = 27.0^{+3.8}_{-3.0}$					
<i>B</i>	0.44	1.0	$0.52 \pm 0.04$	$52^{+8}_{-7}$	$4.4^{+0.8}_{-0.7}$
<i>R</i>	0.64	1.0	$0.54 \pm 0.04$	$50^{+8}_{-7}$	$4.2^{+0.7}_{-0.6}$
IRAC	3.6	1.0	$0.55 \pm 0.04$	$49^{+8}_{-6}$	$4.1^{+0.7}_{-0.6}$
IRAC	3.6	$0.56^{+0.23}_{-0.17}$	$0.63^{+0.06}_{-0.05}$	$43^{+7}_{-6}$	$3.6^{+0.7}_{-0.6}$

**Table 7.** Historical M31 Nova Rate Estimates

Authors	Years	Filter	Novae	Rate
Hubble (1929)	1909 – 1927	<i>B</i>	85	$\sim 30$
Arp (1956)	1953 – 1954	<i>B</i>	30	$26 \pm 4$
Capaccioli et al. (1989) <sup>a</sup>	1955 – 1986	<i>U, B</i>	142	$29 \pm 4$
Shafter & Irby (2001)	1990 – 1997	H $\alpha$	72	$37^{+12}_{-8}$
Darnley et al. (2006, 2004)	1999 – 2003	<i>r', i', g'</i>	20	$65^{+16}_{-15}$
Soraisam et al. (2016)	...	...	...	$\sim 106$
Chen et al. (2016)	...	...	...	$\sim 97$
This work ( $\theta = 1$ )	1995 – 2016	H $\alpha$	253	$48^{+5}_{-4}$
This work ( $\theta = 0.56$ )	1995 – 2016	H $\alpha$	253	$40^{+5}_{-4}$

<sup>a</sup>Based on observations from Rosino (1964), Rosino (1973), and Rosino et al. (1989).

(Darnley et al. 2006) becoming the currently accepted value.

Within the past decade, the observation of several faint, but rapidly fading novae in M31 (Kasliwal et al. 2011), along with the discovery of the remarkable recurrent nova M31N 2008-12a (Shafter et al. 2012; Tang et al. 2014; Darnley et al. 2014; Henze et al. 2014) with its recurrence time of only a year, have fueled speculation that a significant population of faint and rapidly evolving (i.e., “fast”) novae might have been missed in most nova surveys. If so, the nova rate in M31, and other galaxies for that matter, could be significantly

higher than had been measured previously. Following up on this possibility, two recent studies attempted to take this putative population of faint and fast novae into account, finding that M31’s nova rate could be as high as 100 per year.

In one such study, Chen et al. (2016) computed population synthesis models estimating nova rates in galaxies with differing star formation histories and morphological types. In the case of M31, they estimated a global nova rate of  $97 \text{ yr}^{-1}$ . In another study, Soraisam et al. (2016) attempted to correct the nova rates that had been based on the earlier nova surveys of Arp (1956) and Darnley

et al. (2006) for their potential bias against the discovery of faint and fast novae. Based on these corrections, they estimated a global nova rate for M31 of order 106 per year.

Despite the increased spatial and temporal coverage of M31 and the Galaxy made possible by the contributions of automated surveys like the All-Sky Automated Survey for Supernovae (ASAS-SN, Kochanek et al. 2017) and Palomar’s Zwicky Transient Facility (ZTF, Bellm et al. 2019), the extensive observations of the Galactic bulge from the Optical Gravitational Lensing Experiment (OGLE) survey (e.g., see Mróz et al. 2015), not to mention the ever more comprehensive contributions made by amateur astronomers, compelling observational evidence for a significant population of faint and fast novae has failed to materialize. And now, the results of the comprehensive 20-year survey presented here, where we find an M31 nova rate of  $40_{-4}^{+5} \text{ yr}^{-1}$ , similarly provides no support for a population of faint and fast novae. Even the mean of our population-independent ( $\theta = 1$ ) extrapolations, which yields a slightly higher value of  $48_{-3}^{+5} \text{ yr}^{-1}$ , which we consider to provide a firm upper limit on the nova rate in M31, does not suggest the presence of a stealth population of hitherto undiscovered novae.

To summarize, regardless of how we choose to perform the extrapolation from the surveyed region of M31 to the entire galaxy, the results of the present study suggests an M31 nova rate that is significantly lower than that found by Darnley et al. (2006), and far below the values estimated by Chen et al. (2016) and Soraisam et al. (2016). Finally, as we noted earlier (see Figure 1), over the 7-year period between 2016 and 2020, the average annual number of nova candidates reported in M31 was  $\sim 36 \text{ yr}^{-1}$ . Thus, a corollary of our analysis is that the intensive coverage of M31 appears to now be detecting almost all of the novae that arise in the galaxy. A caveat is that since not all M31 nova candidates reported annually are spectroscopically confirmed, some objects may actually be Long-Period Variable stars masquerading as novae (e.g., see Shafter et al. 2008; Taneva et al. 2010). If so, the average reported rate may be best considered an upper limit on the true observed nova rate in M31.

### 6.1. Implications for the Galactic Nova Rate

The eruptions of novae are thought to play a significant role in the chemical evolution of the Galaxy (e.g., Kemp et al. 2022; Molaro et al. 2022; Starrfield et al. 2020; Izzo et al. 2015; Lyke 2003). In addition to producing a fraction of the  ${}^7\text{Li}$  and the short-lived isotopes  ${}^{22}\text{Na}$  and  ${}^{26}\text{Al}$ , novae are believed to be important in the production of the CNO isotopes, particularly  ${}^{15}\text{N}$ , where novae may account for a significant fraction of its Galactic abundance (Romano & Matteucci 2003). An accurate knowledge of the nova rate is therefore essential to a full understanding of Galactic chemical evolution.

The nova rate in the Milky Way, like that in M31, has been estimated many times over the years, both through extrapolations of the observed nova rate to the entire Galaxy, and through a comparison of the Milky Way to external galaxies with measured nova rates. Historically, there has been a tension between estimates based upon these two approaches, with the former having resulted in generally higher rates compared with the latter (e.g., see Table 10, De et al. 2021, for a summary). In particular, recent studies based on extrapolation of the observed nova rate (e.g., Shafter 2017; Özdönmez et al. 2018; De et al. 2021) have found Galactic rates of  $50_{-23}^{+31} \text{ yr}^{-1}$ ,  $67_{-17}^{+21} \text{ yr}^{-1}$ , and  $43.7_{-8.7}^{+19.5} \text{ yr}^{-1}$ , respectively<sup>8</sup>, while extragalactic comparisons (e.g., della Valle & Livio 1994; Shafter et al. 2000, 2014) have predicted lower Galactic rates of  $\approx 20 \text{ yr}^{-1}$ ,  $27_{-8}^{+10} \text{ yr}^{-1}$ , and  $\sim 25 \text{ yr}^{-1}$ , respectively.

The discrepancy between the two approaches has diminished recently thanks to the improved spatial and temporal coverage made possible by all-sky surveys such as ASAS-SN and GAIA (Gaia Collaboration et al. 2016). The analysis of data from these surveys has brought the latest Galactic nova rate estimate down to below  $30 \text{ yr}^{-1}$  (Kawash et al. 2021, 2022), which is now in line with the average of those based on extragalactic scalings.

In light of our new and significantly lower estimate of the nova rate in M31, we are in a position to re-determine the Galactic nova rate based on the ratio of the (infrared) luminosities of our Galaxy and M31. The absolute  $K$ -band magnitude of the Galaxy has been estimated by Malhotra et al. (1996) and by Drimmel & Spergel (2001) who found  $M_K = -24.06$  and  $M_K = -24.02$ , respectively. Recalling that  $M_{K,\odot} = 3.27$  gives an average estimate of  $L_K(\text{G}) = 8.4 \times 10^{10} L_{\odot,K}$  for the  $K$ -band luminosity of the Milky Way. Adopting  $L_K(\text{M31}) = 1.2 \times 10^{10} L_{\odot,K}$  determined earlier gives a Milky Way to M31  $K$ -band luminosity ratio,  $L_K(\text{G})/L_K(\text{M31}) = 0.70 \pm 0.10$ , where we have assumed a 10% error in the luminosities of the individual galaxies. This ratio, coupled with our derived M31 nova rate of  $40_{-4}^{+5} \text{ yr}^{-1}$ , yields a global Galactic nova rate of  $R_G = 28_{-4}^{+5} \text{ yr}^{-1}$  for the Milky Way. This value is fully consistent with both earlier extragalactic scaling estimates, and with the recent Galaxy-based estimate of  $26 \pm 5 \text{ yr}^{-1}$  by Kawash et al. (2022). The remarkable agreement among these estimates provides renewed confidence in the accuracy and fidelity of both our Galactic and M31 nova rate determinations.

## 7. SUMMARY AND CONCLUSIONS

The principal conclusions of our extensive survey of novae in M31 can be summarized as follows:

<sup>8</sup> Note that the Özdönmez et al. (2018) rate is for the Galactic disk only. Adding the Galactic bulge estimate of  $13.8 \pm 2.6 \text{ yr}^{-1}$  (Mróz et al. 2015) suggests an overall Galactic nova rate of  $\sim 80 \text{ yr}^{-1}$ .

(1) During the course of a two-decade long survey spanning the years 1995 through 2016 we have discovered or detected a total of 262 novae in M31, 40 of which are previously unreported. Of these, 253 novae were included as part of two homogeneous surveys, survey A (203 novae) and survey B (50 novae). Survey A was conducted with the KPNO/WIYN 0.9-m reflector and covered the central  $20' \times 20'$  field of M31, while survey B employed the KPNO 4-m reflector and covered a larger  $36' \times 36'$  field, also centered on the nucleus of M31.

(2) After correcting for temporal and spatial incompleteness, nova rates of  $R_A = 17.5^{+0.9}_{-0.4}$  and  $R_B = 27.0^{+3.8}_{-3.0}$  were found for the areas covered in survey A and survey B, respectively.

(3) The spatial distributions of the novae discovered in surveys A and B were compared with the background light of M31 in several photometric bands. The nova distributions follow the galaxy's light reasonably well, with the best fits achieved using the near infrared IRAC  $3.6\mu$  light as given by Model P of Courteau et al. (2011).

(4) The nova rates in the surveyed regions were extrapolated to the entire galaxy by using the ratio of M31's total infrared  $3.6\mu$  light to that contained within the surveyed regions. Two different extrapolations were considered: A population-independent extrapolation assuming that the nova density in M31 was the same in M31's bulge and disk (i.e.,  $\theta [= \rho_d/\rho_b] = 1$ ), and a population-dependent extrapolation based on a maximum likelihood analysis showing that the bulge nova density exceeds that of the disk ( $\theta [= \rho_d/\rho_b] = 0.56^{+0.23}_{-0.17}$ ).

Our population-dependent extrapolation, which we have argued is appropriate for M31, leads to a global nova rate of  $R_{M31} = 40^{+5}_{-4} \text{ yr}^{-1}$ . The population-independent extrapolation ( $\theta=1$ ), which assumes a larger disk nova contribution, gives a somewhat higher rate of  $R_{M31} = 48^{+5}_{-3} \text{ yr}^{-1}$ , and can be considered as providing an upper limit to the nova rate in M31. Both rates are significantly lower than that found by Darnley et al. (2006), and more in line with earlier estimates of M31's nova rate (e.g.,  $37^{+12}_{-8} \text{ yr}^{-1}$ , Shafter & Irby 2001).

(5) When normalized to the  $K$ -band luminosity of M31, we find a luminosity-specific nova rate of  $3.3 \pm 0.4$  novae per year per  $10^{10}$  solar luminosities in the  $K$  band, which is typical of other galaxies with measured nova rates.

(6) Our new determination of the nova rate in M31, which is based upon the largest sample of novae ever used in a single study of this galaxy, is inconsistent with recent suggestions (e.g., Soraisam et al. 2016; Chen et al. 2016) that the nova rate in M31 (and the Galaxy) might approach  $100 \text{ yr}^{-1}$ . As a corollary, we find no evidence for the existence of a significant population of faint and fast novae such as M31N 2008-12a.

(7) Scaling our M31 nova rate to the Milky Way using the relative  $K$ -band luminosities of each galaxy, we estimate a Galactic nova rate of  $R_G = 28^{+5}_{-4} \text{ yr}^{-1}$ .

We conclude on a optimistic note that after more than a century of observations and the discovery of  $\sim 500$  novae in the Galaxy and  $\sim 1300$  in M31, the annual rates of novae in these two galaxies appear to now be well constrained and mutually consistent. Future observations should be directed at better understanding the role the underlying stellar population plays in determining the properties of emergent novae.

We would like to thank the referee, Massimo Della Valle, for several insightful suggestions that helped improve the presentation of our results.

The work presented here is based in part on observations at Kitt Peak National Observatory at NSF's NOIRLab, which is managed by the Association of Universities for Research in Astronomy (AURA) under a cooperative agreement with the National Science Foundation. The authors are honored to be permitted to conduct astronomical research on Iolkam Du'ag (Kitt Peak), a mountain with particular significance to the Tohono O'odham. This paper is dedicated to the firefighters who saved the telescopes on Kitt Peak during the Contreras Fire in June 2022.

We are indebted to the many thousands of teachers and students who have participated in this project as part of the RBSE, TLRBSE, and RBSE-U programs, the names of whom are too many to list.

This material is based upon work supported by the National Science Foundation under Grant Nos. ESIE-9619028, ESIE-0101982, DUE-0618441, DUE-0618849, and DUE-0920293. Any opinions, findings, and conclusions or recommendations expressed in this material are those of the authors and do not necessarily reflect the views of the National Science Foundation.

D.L. Corbett, M. Rene, and D. Hernandez were supported through a NASA grant awarded to the Arizona/NASA Space Grant Consortium. The material contained in this document is based upon work supported by a National Aeronautics and Space Administration (NASA) grant or cooperative agreement. Any opinions, findings, conclusions or recommendations expressed in this material are those of the author and do not necessarily reflect the views of NASA.

*Facilities:* WIYN:0.9-m, Mayall, Bok, KPNO:2.1-m, McGraw-Hill

*Software:* IRAF (Tody 1986), SAOImageDS9 (Joye & Mandel 2003), Astropy (Astropy Collaboration et al. 2013, 2018)

## REFERENCES

- Arp, H. C. 1956, *AJ*, 61, 15, doi: [10.1086/107284](https://doi.org/10.1086/107284)
- Astropy Collaboration, Robitaille, T. P., Tollerud, E. J., et al. 2013, *A&A*, 558, A33, doi: [10.1051/0004-6361/201322068](https://doi.org/10.1051/0004-6361/201322068)
- Astropy Collaboration, Price-Whelan, A. M., Sipőcz, B. M., et al. 2018, *AJ*, 156, 123, doi: [10.3847/1538-3881/aabc4f](https://doi.org/10.3847/1538-3881/aabc4f)
- Barmby, P., Ashby, M. L. N., Bianchi, L., et al. 2006, *ApJL*, 650, L45, doi: [10.1086/508626](https://doi.org/10.1086/508626)
- Bellm, E. C., Kulkarni, S. R., Graham, M. J., et al. 2019, *PASP*, 131, 018002, doi: [10.1088/1538-3873/aaecbe](https://doi.org/10.1088/1538-3873/aaecbe)
- Capaccioli, M., Della Valle, M., D’Onofrio, M., & Rosino, L. 1989, *AJ*, 97, 1622, doi: [10.1086/115104](https://doi.org/10.1086/115104)
- Chen, H.-L., Woods, T. E., Yungelson, L. R., Gilfanov, M., & Han, Z. 2016, *MNRAS*, 458, 2916, doi: [10.1093/mnras/stw458](https://doi.org/10.1093/mnras/stw458)
- Ciardullo, R., Ford, H. C., Neill, J. D., Jacoby, G. H., & Shafter, A. W. 1987, *ApJ*, 318, 520, doi: [10.1086/165388](https://doi.org/10.1086/165388)
- Ciardullo, R., Shafter, A. W., Ford, H. C., et al. 1990, *ApJ*, 356, 472, doi: [10.1086/168855](https://doi.org/10.1086/168855)
- Coelho, E. A., Shafter, A. W., & Misselt, K. A. 2008, *ApJ*, 686, 1261, doi: [10.1086/591517](https://doi.org/10.1086/591517)
- Courteau, S., Widrow, L. M., McDonald, M., et al. 2011, *ApJ*, 739, 20, doi: [10.1088/0004-637X/739/1/20](https://doi.org/10.1088/0004-637X/739/1/20)
- Darnley, M. J., Williams, S. C., Bode, M. F., et al. 2014, *A&A*, 563, L9, doi: [10.1051/0004-6361/201423411](https://doi.org/10.1051/0004-6361/201423411)
- Darnley, M. J., Bode, M. F., Kerins, E., et al. 2004, *MNRAS*, 353, 571, doi: [10.1111/j.1365-2966.2004.08087.x](https://doi.org/10.1111/j.1365-2966.2004.08087.x)
- . 2006, *MNRAS*, 369, 257, doi: [10.1111/j.1365-2966.2006.10297.x](https://doi.org/10.1111/j.1365-2966.2006.10297.x)
- De, K., Kasliwal, M. M., Hankins, M. J., et al. 2021, *ApJ*, 912, 19, doi: [10.3847/1538-4357/abeb75](https://doi.org/10.3847/1538-4357/abeb75)
- de Vaucouleurs, G. 1958, *ApJ*, 128, 465, doi: [10.1086/146564](https://doi.org/10.1086/146564)
- Della Valle, M., & Izzo, L. 2020, *A&A Rv*, 28, 3, doi: [10.1007/s00159-020-0124-6](https://doi.org/10.1007/s00159-020-0124-6)
- della Valle, M., & Livio, M. 1994, *A&A*, 286, 786
- Della Valle, M., & Livio, M. 1998, *ApJ*, 506, 818, doi: [10.1086/306275](https://doi.org/10.1086/306275)
- della Valle, M., Rosino, L., Bianchini, A., & Livio, M. 1994, *A&A*, 287, 403
- Drimmel, R., & Spergel, D. N. 2001, *ApJ*, 556, 181, doi: [10.1086/321556](https://doi.org/10.1086/321556)
- Fazio, G. G., Hora, J. L., Allen, L. E., et al. 2004, *ApJS*, 154, 10, doi: [10.1086/422843](https://doi.org/10.1086/422843)
- Franck, J. R., Shafter, A. W., Hornoch, K., & Misselt, K. A. 2012, *ApJ*, 760, 13, doi: [10.1088/0004-637X/760/1/13](https://doi.org/10.1088/0004-637X/760/1/13)
- Freedman, W. L., Madore, B. F., Gibson, B. K., et al. 2001, *ApJ*, 553, 47, doi: [10.1086/320638](https://doi.org/10.1086/320638)
- Gaia Collaboration, Prusti, T., de Bruijne, J. H. J., et al. 2016, *A&A*, 595, A1, doi: [10.1051/0004-6361/201629272](https://doi.org/10.1051/0004-6361/201629272)
- Güth, T., Shafter, A. W., & Misselt, K. A. 2010, *ApJ*, 720, 1155, doi: [10.1088/0004-637X/720/2/1155](https://doi.org/10.1088/0004-637X/720/2/1155)
- Hatano, K., Branch, D., Fisher, A., & Starrfield, S. 1997, *ApJL*, 487, L45, doi: [10.1086/310862](https://doi.org/10.1086/310862)
- Henze, M., Ness, J. U., Darnley, M. J., et al. 2014, *A&A*, 563, L8, doi: [10.1051/0004-6361/201423410](https://doi.org/10.1051/0004-6361/201423410)
- Hubble, E. P. 1929, *ApJ*, 69, 103, doi: [10.1086/143167](https://doi.org/10.1086/143167)
- Izzo, L., Della Valle, M., Mason, E., et al. 2015, *ApJL*, 808, L14, doi: [10.1088/2041-8205/808/1/L14](https://doi.org/10.1088/2041-8205/808/1/L14)
- Jarrett, T. H., Chester, T., Cutri, R., Schneider, S. E., & Huchra, J. P. 2003, *AJ*, 125, 525, doi: [10.1086/345794](https://doi.org/10.1086/345794)
- Joye, W. A., & Mandel, E. 2003, in *Astronomical Society of the Pacific Conference Series*, Vol. 295, *Astronomical Data Analysis Software and Systems XII*, ed. H. E. Payne, R. I. Jedrzejewski, & R. N. Hook, 489
- Kasliwal, M. M., Cenko, S. B., Kulkarni, S. R., et al. 2011, *ApJ*, 735, 94, doi: [10.1088/0004-637X/735/2/94](https://doi.org/10.1088/0004-637X/735/2/94)
- Kato, M., Saio, H., Hachisu, I., & Nomoto, K. 2014, *ApJ*, 793, 136, doi: [10.1088/0004-637X/793/2/136](https://doi.org/10.1088/0004-637X/793/2/136)
- Kaur, A. 2016, PhD thesis, Clemson University, South Carolina
- Kawash, A., Chomiuk, L., Rodriguez, J. A., et al. 2021, *ApJ*, 922, 25, doi: [10.3847/1538-4357/ac1fla](https://doi.org/10.3847/1538-4357/ac1fla)
- Kawash, A., Chomiuk, L., Strader, J., et al. 2022, arXiv e-prints, arXiv:2206.14132, <https://arxiv.org/abs/2206.14132>
- Kemp, A. J., Karakas, A. I., Casey, A. R., et al. 2022, *ApJL*, 933, L30, doi: [10.3847/2041-8213/ac7c72](https://doi.org/10.3847/2041-8213/ac7c72)
- Kent, S. M. 1987, *AJ*, 94, 306, doi: [10.1086/114472](https://doi.org/10.1086/114472)
- Kochanek, C. S., Shappee, B. J., Stanek, K. Z., et al. 2017, *PASP*, 129, 104502, doi: [10.1088/1538-3873/aa80d9](https://doi.org/10.1088/1538-3873/aa80d9)
- Lyke, J. E. 2003, PhD thesis, University of Minnesota, Twin Cities
- Malhotra, S., Spergel, D. N., Rhoads, J. E., & Li, J. 1996, *ApJ*, 473, 687, doi: [10.1086/178181](https://doi.org/10.1086/178181)
- Massey, P., McNeill, R. T., Olsen, K. A. G., et al. 2007, *AJ*, 134, 2474, doi: [10.1086/523658](https://doi.org/10.1086/523658)
- Massey, P., Olsen, K. A. G., Hodge, P. W., et al. 2006, *AJ*, 131, 2478, doi: [10.1086/503256](https://doi.org/10.1086/503256)
- Molaro, P., Izzo, L., D’Odorico, V., et al. 2022, *MNRAS*, 509, 3258, doi: [10.1093/mnras/stab3106](https://doi.org/10.1093/mnras/stab3106)
- Monet, D. G., Levine, S. E., Canzian, B., et al. 2003, *AJ*, 125, 984, doi: [10.1086/345888](https://doi.org/10.1086/345888)
- Mróz, P., Udalski, A., Poleski, R., et al. 2015, *ApJS*, 219, 26, doi: [10.1088/0067-0049/219/2/26](https://doi.org/10.1088/0067-0049/219/2/26)
- Neill, J. D., & Shara, M. M. 2004, *AJ*, 127, 816, doi: [10.1086/381484](https://doi.org/10.1086/381484)

- Nomoto, K. 1982, *ApJ*, 253, 798, doi: [10.1086/159682](https://doi.org/10.1086/159682)
- Özdönmez, A., Ege, E., Güver, T., & Ak, T. 2018, *MNRAS*, 476, 4162, doi: [10.1093/mnras/sty432](https://doi.org/10.1093/mnras/sty432)
- Peng, C. Y., Ho, L. C., Impey, C. D., & Rix, H.-W. 2002, *AJ*, 124, 266, doi: [10.1086/340952](https://doi.org/10.1086/340952)
- Rector, T. A., Puckett, A. W., Wooten, M. M., et al. 2019, in *Astronomy Education*, Volume 1, 2514-3433 (IOP Publishing), 7–1 to 7–10, doi: [10.1088/2514-3433/ab2b42ch7](https://doi.org/10.1088/2514-3433/ab2b42ch7)
- Ritchey, G. W. 1917, *PASP*, 29, 210, doi: [10.1086/122638](https://doi.org/10.1086/122638)
- Romano, D., & Matteucci, F. 2003, *MNRAS*, 342, 185, doi: [10.1046/j.1365-8711.2003.06526.x](https://doi.org/10.1046/j.1365-8711.2003.06526.x)
- Rosino, L. 1964, *Annales d'Astrophysique*, 27, 498
- . 1973, *A&AS*, 9, 347
- Rosino, L., Capaccioli, M., D'Onofrio, M., & della Valle, M. 1989, *AJ*, 97, 83, doi: [10.1086/114959](https://doi.org/10.1086/114959)
- Shafter, A. W. 2017, *ApJ*, 834, 196, doi: [10.3847/1538-4357/834/2/196](https://doi.org/10.3847/1538-4357/834/2/196)
- . 2019, *Extragalactic Novae; A historical perspective*, doi: [10.1088/2514-3433/ab2c63](https://doi.org/10.1088/2514-3433/ab2c63)
- Shafter, A. W., Ciardullo, R., & Pritchett, C. J. 2000, *ApJ*, 530, 193, doi: [10.1086/308349](https://doi.org/10.1086/308349)
- Shafter, A. W., Curtin, C., Pritchett, C. J., Bode, M. F., & Darnley, M. J. 2014, in *Astronomical Society of the Pacific Conference Series*, Vol. 490, *Stellar Novae: Past and Future Decades*, ed. P. A. Woudt & V. A. R. M. Ribeiro, 77. <https://arxiv.org/abs/1307.2296>
- Shafter, A. W., Hornoch, K., Ciardullo, J. V. R., Darnley, M. J., & Bode, M. F. 2012, *The Astronomer's Telegram*, 4503, 1
- Shafter, A. W., & Irby, B. K. 2001, *ApJ*, 563, 749, doi: [10.1086/324044](https://doi.org/10.1086/324044)
- Shafter, A. W., Kundu, A., & Henze, M. 2017, *Research Notes of the American Astronomical Society*, 1, 11, doi: [10.3847/2515-5172/aa9847](https://doi.org/10.3847/2515-5172/aa9847)
- Shafter, A. W., Rau, A., Quimby, R. M., et al. 2009, *ApJ*, 690, 1148, doi: [10.1088/0004-637X/690/2/1148](https://doi.org/10.1088/0004-637X/690/2/1148)
- Shafter, A. W., Ciardullo, R., Burwitz, V., et al. 2008, *The Astronomer's Telegram*, 1851, 1
- Shafter, A. W., Darnley, M. J., Hornoch, K., et al. 2011, *ApJ*, 734, 12, doi: [10.1088/0004-637X/734/1/12](https://doi.org/10.1088/0004-637X/734/1/12)
- Shafter, A. W., Hornoch, K., Benáček, J., et al. 2021, *ApJ*, 923, 239, doi: [10.3847/1538-4357/ac2c79](https://doi.org/10.3847/1538-4357/ac2c79)
- Shara, M. M., Doyle, T. F., Lauer, T. R., et al. 2016, *ApJS*, 227, 1, doi: [10.3847/0067-0049/227/1/1](https://doi.org/10.3847/0067-0049/227/1/1)
- Soraisam, M. D., Gilfanov, M., Wolf, W. M., & Bildsten, L. 2016, *MNRAS*, 455, 668, doi: [10.1093/mnras/stv2359](https://doi.org/10.1093/mnras/stv2359)
- Soraisam, M. D., Gilfanov, M., Kupfer, T., et al. 2017, *A&A*, 599, A48, doi: [10.1051/0004-6361/201629368](https://doi.org/10.1051/0004-6361/201629368)
- Starrfield, S., Bose, M., Iliadis, C., et al. 2020, *ApJ*, 895, 70, doi: [10.3847/1538-4357/ab8d23](https://doi.org/10.3847/1538-4357/ab8d23)
- Starrfield, S., Iliadis, C., & Hix, W. R. 2016, *PASP*, 128, 051001, doi: [10.1088/1538-3873/128/963/051001](https://doi.org/10.1088/1538-3873/128/963/051001)
- Taneva, N., Valcheva, A., Ovcharov, E., & Nedialkov, P. 2010, *Bulgarian Astronomical Journal*, 14, 54
- Tang, S., Bildsten, L., Wolf, W. M., et al. 2014, *ApJ*, 786, 61, doi: [10.1088/0004-637X/786/1/61](https://doi.org/10.1088/0004-637X/786/1/61)
- Tody, D. 1986, in *Society of Photo-Optical Instrumentation Engineers (SPIE) Conference Series*, Vol. 627, *Instrumentation in astronomy VI*, ed. D. L. Crawford, 733, doi: [10.1117/12.968154](https://doi.org/10.1117/12.968154)
- Townsley, D. M., & Bildsten, L. 2005, *ApJ*, 628, 395, doi: [10.1086/430594](https://doi.org/10.1086/430594)
- Warner, B. 1995, *Cataclysmic variable stars*, Vol. 28
- Williams, R. E. 1992, *AJ*, 104, 725, doi: [10.1086/116268](https://doi.org/10.1086/116268)
- Williams, S. J., & Shafter, A. W. 2004, *ApJ*, 612, 867, doi: [10.1086/422833](https://doi.org/10.1086/422833)
- Willmer, C. N. A. 2018, *ApJS*, 236, 47, doi: [10.3847/1538-4365/aabfdf](https://doi.org/10.3847/1538-4365/aabfdf)
- Wooten, M. M., Coble, K., Puckett, A. W., & Rector, T. 2018, *Phys. Rev. Phys. Educ. Res.*, 14, 010151, doi: [10.1103/PhysRevPhysEducRes.14.010151](https://doi.org/10.1103/PhysRevPhysEducRes.14.010151)